AN EXPERIMENTAL INVESTIGATION OF STANDING VORTICES IN AN OPEN CAVITY

ROGER L. BENNETT

AN EXPERIMENTAL INVESTIGATION OF STANDING VORTICES IN AN OPEN CAVITY

by

Roger L. Bennett
Lieutenant, United States Navy
B.S., United States Naval Academy, 1960

Submitted in partial fulfillment of the
requirements for the degree of

MASTER OF SCIENCE IN MECHANICAL ENGINEERING

from the

NAVAL POSTGRADUATE SCHOOL
June 1967

ABSTRACT

This report describes the measurement of velocity profiles within and directly above a rectangular cavity with air flow across its mouth, such that standing vortices are induced in the cavity. The constant temperature hot-wire anemometer was used to determine velocity profiles at 75 feet per second free stream velocity and cavity depth over length ratios of 0.75 and 1.0. Both three-dimensional and cavity geometry effects were exhibited for the vortices, and lack of periodicity in the velocities was consistently noted.

All of the experimental work was conducted during April and May 1967, at the Naval Postgraduate School.

TABLE OF CONTENTS

LIST OF ILLUSTRATIONS

TABLE OF SYMBOLS

C	a constant
D	cavity depth (in)
L	cavity length (in)
q	dynamic head (lbs/sq. ft) = $\frac{1}{2}\rho U^2$
T	temperature (degrees Fahrenheit)
u	mean velocity (ft/sec)
$\underline{u}$	mean velocity ratio (u/U)
U	reference free stream velocity (ft/sec)
u_r	root mean square value of velocity turbulence (ft/sec)
$\underline{u}_r$	turbulence velocity ratio (u_r/U)
W	cavity width (in)
x	coordinate, distance in flow direction from upstream wall of cavity (in)
y	coordinate, vertical distance from cavity floor (in)
z	coordinate, horizontal distance in direction transverse to flow measured from left side of cavity looking downstream (in)
ρ (rho)	air density (slugs/cubic foot)
ω (omega)	uncertainty (percent)
1	as subscript, denoting x direction
2	as subscript, denoting y direction

ACKNOWLEDGEMENT

The author is much indebted to Professor Louis V. Schmidt for inspiration and guidance leading toward and throughout the conduct of this investigation. Appreciation is also expressed to Professor P. F. Pucci for assistance. Grateful acknowledgement is also due Mr. S. Johnson and Mr. T. Dunton for their work in construction, assembly, and installation of the experimental equipment.

1. Introduction

Since the advent of high speed aircraft and ships, increasing interest has been generated in the nature of the effects of discontinuities in the boundary surfaces of the fluid flow fields. Cavity-type discontinuities, such as bomb bays and landing gear wells in aircraft and sea water injection openings in ships, have been observed to contain strong periodically fluctuating pressure fields which can attain intensities sufficient to induce significant dynamic response of the structure and/or the vehicle. Because of these disturbing effects, cavity-type discontinuities have received particular attention.

Prior efforts have associated the observed phenomena with Helmholz cavity resonance, discovered by Helmholz, who worked out formal analytical expressions. Rayleigh, in the late 19th century extended Helmholz's work using energy relations to allow end corrections for different geometries. At present the information on the boundary conditions of the cavity systems is insufficient to make use of the results practical.

In 1944, Tillman (12) published the results of tests which determined the drag coefficients of various surface irregularities including rectangular and circular cross-section cavities. Blokhintsev (1) initiated modern investigations of flow-excited cavity resonance in 1945.

During the 1950's, Roshko (8,9) and Krishnamurty (6) published results of experiments conducted at the California Institute of Technology. These works presented information on

the pressure distributions on the cavity walls, pressure drag and friction coefficient, and acoustic radiation from the cavities. Dependence of the quantities on geometric and flow parameters was included. Roshko's work also contained a brief presentation of estimated vortex velocities within the cavity, based on measurements near the walls.

Harrington (4), in 1957, addressed the Acoustical Society of America on the mechanism of cavity resonances. Since 1960, Dunham (2) and Rossiter (10) have published results of studies of flow over two-dimensional cavities.

It should be noted, however, that none of the previous investigations penetrated the cavity interior but, rather, confined themselves to effects at the cavity mouth or within a very close distance from the walls. Further, all prior efforts have been based on the assumption that end effects could be ignored, hence the frequent references to "two-dimensional" cavities.

Roshko (9) discussed difficulties to be encountered in extending investigations toward the vortex centers, relating the problems to the relative magnitudes of the turbulence and low mean velocities at the core.

Inasmuch as this discussion took place in 1953, before reliable constant temperature hot-wire anemometer circuitry was available, it was felt that the difficulties could be overcome and that a significant advancement of the knowledge of cavity resonance might be afforded by results of observation of the vortex velocities and frequencies of oscillation

throughout the cavity, and comparisons of the observed quantities for varying cavity geometries. In particular, it was felt that a beginning for the determination of the influence of boundary conditions could result from this work. A further purpose of these studies was to identify any dominant frequencies of vortex oscillation relative to the characteristic geometric parameters of the cavity (such as length and depth) and to the free stream tunnel velocity.

Definite frequencies were not observed so that in final form, the objectives of the investigation were reduced to a study of the vortex velocity distributions and their reaction to variable cavity geometry.

2. Summary of Theory

As noted previously, analytical investigation of the flow induced forced vortex in a cavity has been hampered by ignorance of the boundary conditions. The forced vortex is generally associated with flow of a fluid in a container revolving about a central axis, so that linear velocities are directly a function of radius from the axis of rotation out to the container wall, (see 11).

In the flow induced case, however, the fluid velocities are only roughly a function of radius from the vortex center, being functions also of coordinates originating at the walls and in the free stream. Therefore the mechanism of vortex formation in an open cavity has only been described by the results of experimental observations.

In shallow cavities, as described by Rossiter (10), flow through the cavity may be considered as flow down and up a step at the upstream and downstream walls respectively (see Figure 1).

Figure 1 Shallow cavity flow with no vortex formed

These step changes will be accompanied by a pressure drop in the fluid as it separates from the cavity's upstream edge and a pressure rise on the cavity floor where the flow reattaches itself. Near the rear wall, flow will be retarded and pressure

will rise until the boundary layer separates and forms a high pressure region at the downstream wall of the cavity. As the depth/length (D/L) ratio of the cavity is increased, the attachment and separation points on the cavity floor move together until coincident. Any further increase in D/L ratio results in reverse flow from the high pressure to the low pressure areas and a captive vortex is formed, as shown in Figure 2.

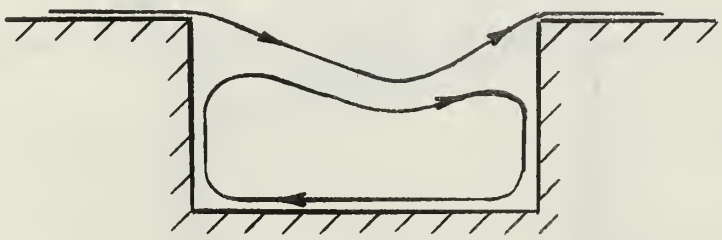

Figure 2 Standing vortex formed

Dunham (2) has proposed that cavity oscillation is activated by the presence of an inflection point in the mixing zone, which causes separation when forced into a positive pressure gradient. Figure 3 shows the streamline pattern prior to oscillation.

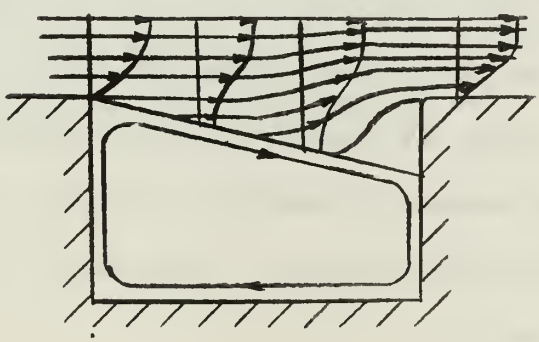

Figure 3 Streamline pattern of flow before oscillation occurs

As velocity increases beyond the leading edge of the cavity and is accompanied by a pressure drop, a positive pressure gradient forms over the after portion of the cavity mouth in front of the stagnation region on the downstream wall. A vortex, caused by flow separation, will form in the boundary layer (see Figure 4).

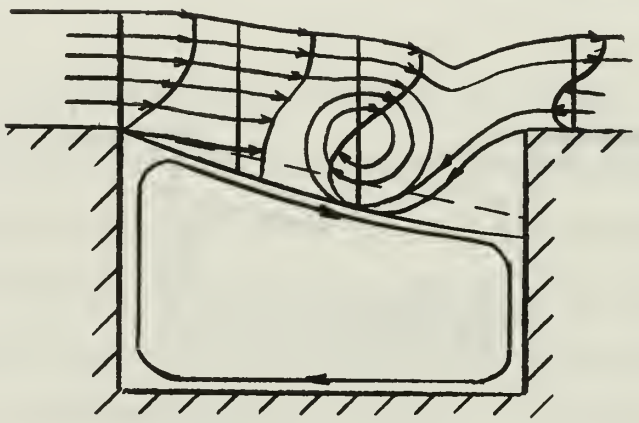

Figure 4 Streamline pattern showing vortex in the boundary layer

At the point shown the cavity volume has been compressed.

After formation of the vortex, the positive pressure gradient in the cavity is destroyed and the vortex moves to the downstream lip. When the vortex strikes the lip, the inward portion of the velocity field is redirected into the downstream boundary layer while the outward portion entrains fluid in the cavity mouth and causes a pressure reduction over the downstream lip of the cavity (see Figure 5). The cavity volume is here seen to have expanded.

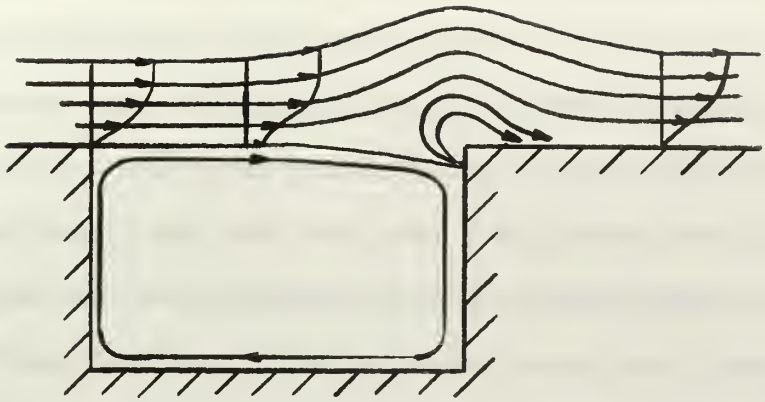

Figure 5 Streamline pattern as boundary layer vortex strikes the downstream lip

Once the vortex has passed into the boundary layer, flow returns to the streamline pattern of Figure 3.

The effective cavity volume thus oscillates about an initial undisturbed volume, emitting periodic radiations into the free stream. As determined by Krishnamurty (6), the frequencies of these radiations are dependent on flow Mach number and, hence, could be used to determine local Mach numbers in the supersonic range when other measuring devices might be difficult to use. Krishnamurty's report (6), also raised the question of the effect of a turbulent boundary layer ahead of the cavity, suggesting that it could produce a different wave system.

3. Description of Apparatus and Instrumentation

A. Apparatus

Apparatus used in conducting this investigation consisted of a) the wind tunnel and controls, b) the test cavity, c) the hot wire probe, and d) the traverse mechanism.

The wind tunnel used was built for the Naval Postgraduate School by West Coast Research Corporation of Los Angeles, California. The tunnel contains a 10 foot square entrance section ahead of a 3.5 by 5.0 foot test section 7.5 feet long, followed by 20 feet of diffuser section. The downstream end of the test section was vented to the atmosphere. Wind speed was controlled by varying the pitch of the fan blades. The fan was turned by a Brook A.C. induction motor, model 203/103A supplied with 60 cycle 3 phase 500 volt power from the building supply. The motor delivered up to 150 horsepower at approximately 1170 RPM.

Tunnel wind speed was observed on a two meter differential water manometer graduated in 0.01 centimeter increments. Pressure from a static pressure ring located at the entrance to the test section was led to the top of the manometer. Pressure from a shrouded total head pitot tube, also located at the entrance to the test section, was led to the top of the fluid reservoir, so that fluid level in the manometer represented the pressure difference between stagnation and static pressures at the entrance to the test section, which was related by a previous tunnel calibration to tunnel dynamic pressure, q.

The test cavity corresponded to a variable depth cutout 4 inches long by 12 inches wide relative to the flow (see Figure 7). The cavity walls were mounted to a baseplate which was in turn mounted on the floor of the tunnel test section and faired to the tunnel floor 2 feet ahead of the cavity's upstream lip. The floor of the cavity was designed to be set at any depth between 0 and 8 inches. Grooves in the floor permitted traversing the hot wire probe. During operation, these grooves were sealed by slot pieces which were introduced through cutouts in the sides of the cavity. Half-inch plexiglass was used for all pieces.

The hot wire probe consisted of an 0.25 inch diameter steel tube, 17 inches long, with 0.005 by 0.015 by 0.5 inch jewelers broaches imbedded in epoxy at one end of the tube and an Amphenol 3016A-12S-3S socket at the other end. The 0.00015 inch diameter tungsten hot wire was soldered between the tips of the broaches. The socket provided a terminal for leads to the anemometer.

The traverse mechanism was constructed of 2 inch O.D. by 1-5/8 inch I.D. rolled aluminum tubing, 9.5 inches long (see Figure 7). This tube was plugged at one end, the plug containing an 0.25 inch hole aligned with the tube axis to provide passage and guidance for the probe. The probe was supported by a postioning piston which had ears extending through grooves in the cylinder wall. The piston ears rested on a postioning ring which was threaded at 10 threads per inch, as was the lower 7 inches of the outside cylinder wall.

The cylinder was supported on four 0.25 inch rods which passed through the top of the cylinder and plug. Two of the

rods were oriented in the x-direction (parallel to flow) and two were oriented in the y-direction (transverse to flow). One rod in each direction was threaded to provide positioning control of the cylinder in the horizontal plane. The rods extended through grooves in a "skirt" around the base of the cavity.

B. Instrumentation

Instrumentation of this investigation consisted of a) the hot wire anemometer, b) an RMS meter, and c) an oscilloscope (reference Figures 6 and 8).

A constant temperature hot wire anemometer, model 200 made by Security Associates Applied Science, Carmel, California, was used. This device contains circuitry to maintain a constant wire temperature by varying its resistance to reflect changes in flow velocity past the wire. The major advantage of the constant temperature hot wire circuit was that the wire was used in the feedback part of the amplifier circuits and hence allowed avoidance of frequency limitations and narrow linear velocity ranges as found in constant current circuits. The linear voltage output relative to air flow speed, makes possible the use of this instrument to measure flow fields which heretofore could not be explored. (Reference (5) contains a particularly good description of the theory on which the hot wire anemometer is based). A self-contained DC meter with a selection of scales (10, 100, or 300 milliamps and 1 or 5 volts) provided mean velocity monitoring. Additionally, velocity fluctuations about the mean were measured at an output jack.

A true RMS vacuum tube voltmeter, model 320A of Ballantine Laboratories, Incorporated, Boonton, New Jersey was used for turbulence measurements. This meter can observe sine, complex, pulse, or random waveforms from 0.1 millivolt to 33 volts with an accuracy of ± 2% of indication for frequencies from 20 cps to 400 kcps.

Waveforms were observed on a Hewlett-Packard Company model 130 C oscilloscope. Measurement bandwidth was 500 kilocycles with horizontal and vertical seneitivity of 200 microvolts per centimeter.

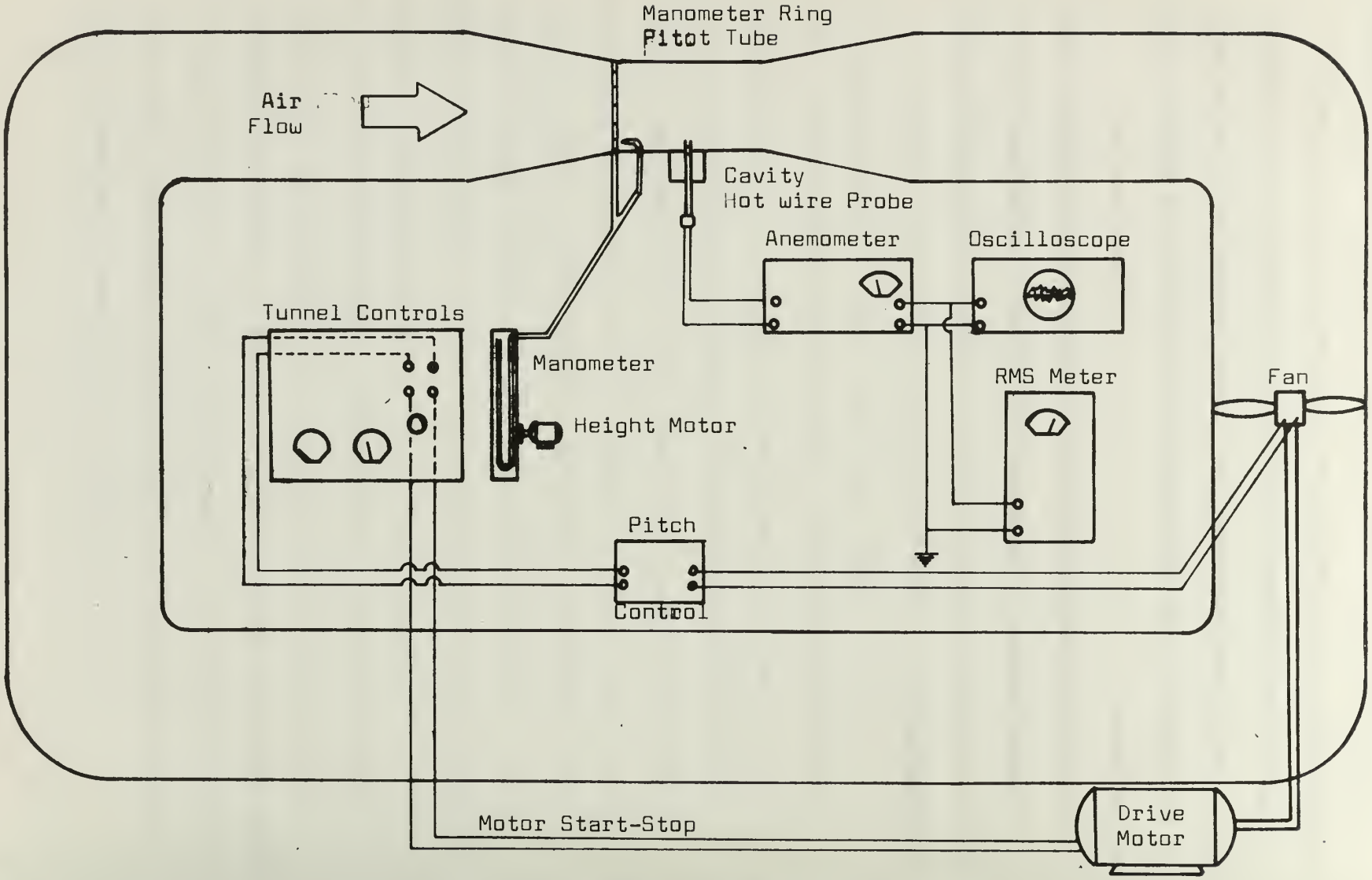

Figure 6 - Schematic, Experimental Layout

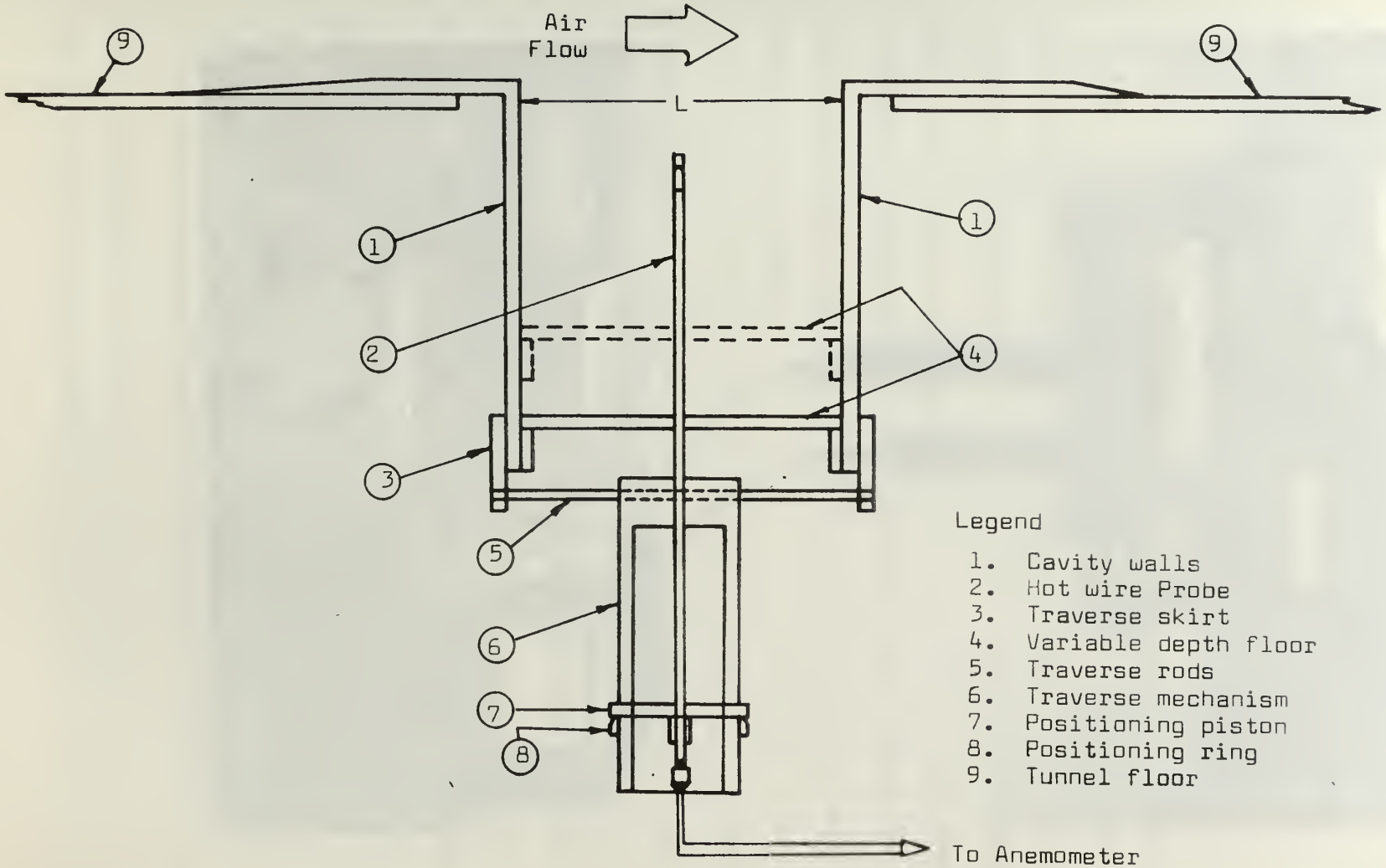

Figure 7 - Schematic, Test Cavity and Traverse Mechanism

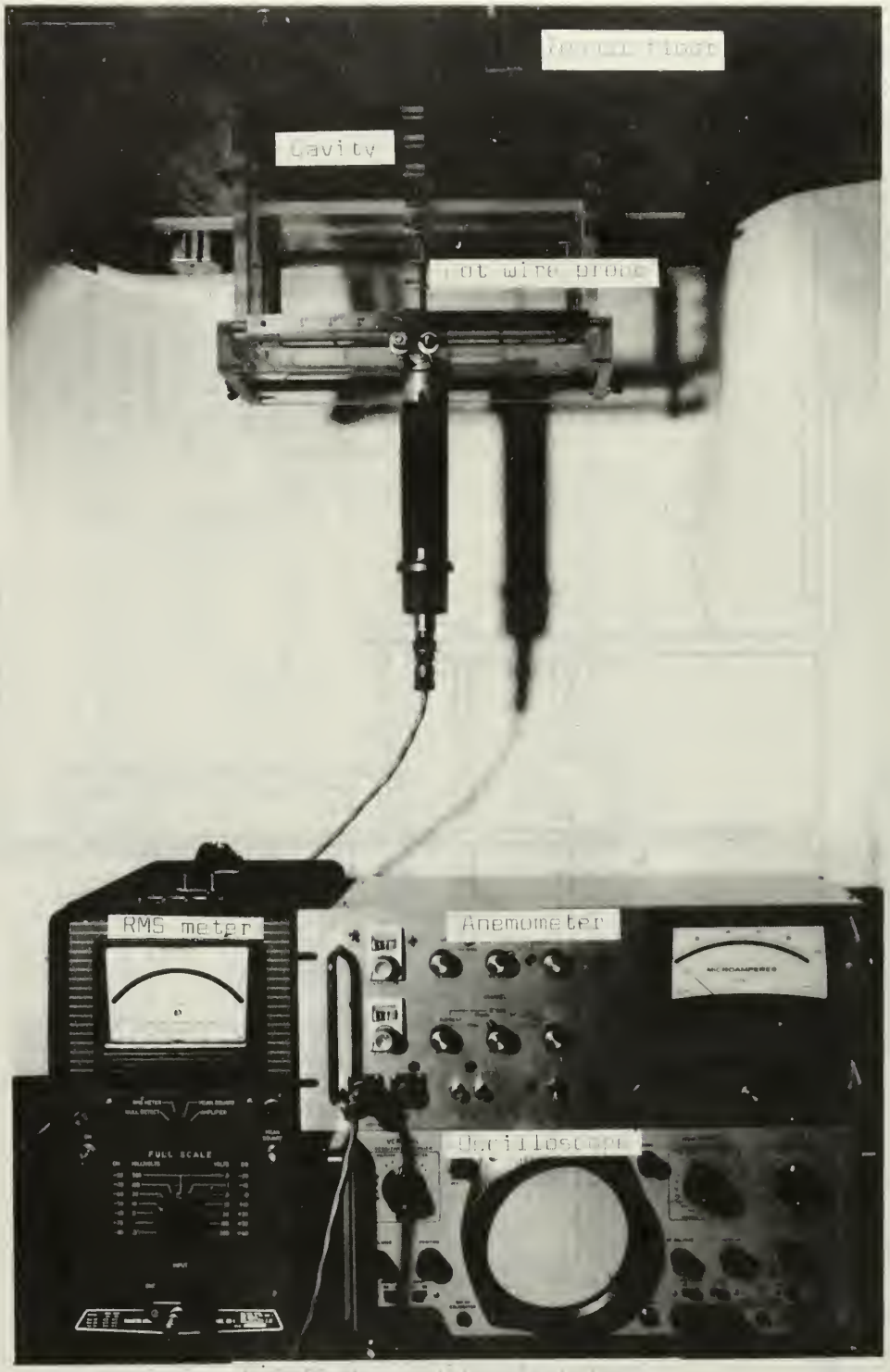
Cavity
Hot wire probe
RMS meter
Anemometer
Oscilloscope

4. Experimental Procedure

This investigation was executed in five steps as follows:

a. establishing the cavity D/L ratio

b. calibrating the anemometer

c. setting the tunnel wind speed

d. positioning the hot wire

e. reading and recording the values of $\underline{u}$ and $\underline{u}_T$

The cavity D/L ratio was set by supporting the moveable cavity floor, at the corners, with wood pieces cut to the desired length. D/L ratios in the vicinity of 1.0 have been observed by Roshko and others to yield single captive vortices, and therefore, D/L ratios of 0.75 and 1.0 were chosen for this investigation. Depth was checked from inside the cavity to insure the setting within ± 0.01 inches.

Calibration of the anemometer was straightforward following the manufacturer's recommendations. With no flow and the attenuator turned fully clockwise, the hot wire resistance was set to give a 25 milliamp reading on the 100 milliamp scale. This established a safe limiting resistance to the wire to prevent wire burnout at low flow rates. Next, with the meter on the one volt scale, the needle was adjusted to zero from the upscale side, after which the attenuator control was turned full counterclockwise to reduce sensitivity. Finally, with the hot wire in position seven inches above the tunnel floor and tunnel wind velocity set to 75 feet per second, the attenuator was adjusted to give a full scale reading, that is, one volt D.C. By so doing, readings on the one volt scale repre-

sented the mean velocity normalized with respect to the free stream velocity. Additionally, the anemometer output represented the fluctuations of velocity about the mean, so that the value of RMS turbulence similarly normalized could be read directly on an RMS meter.

Tunnel wind speed was controlled by varying the pitch of the fan blades to give the desired dynamic pressure, q. For a free stream velocity, U, of 75 feet per second, a q of 6.67 pounds per square foot was calculated. From tunnel calibration curves, q of 6.67 corresponded to 3.32 centimeters of water in the control manometer. This value was set and checked for each run. The value of 75 feet per second for tunnel wind speed was chosen to provide direct comparison of results with those obtained by Roshko (9).

The hot wire was visually aligned transverse to the flow (see Figure 9). Position in the x-y plane was controlled by the horizontal positioning screws of the traverse mechanism. The positioning screws were indexed so that their position opposite a scale on the skirts could be read to ± 0.01 inches. A calibration between positioning screw index reading and wire location was conducted with the setup in the tunnel. This consisted simply of recording index readings and measured wire position.

The wire height was controlled by setting the positioning ring at an indexed zero location and introducing the probe full length. At this position, the wire was measured at seven inches above the tunnel floor. The positioning ring was then lowered

one turn for each 0.1 inch desired height change. Since full ring travel on the cylinder was only seven inches, it was necessary to withdraw the probe after traversing this distance and reposition the ring to zero. The distance withdrawn was measured by dividers and checked by observing the meter readings, since at the height at which the probe had to be withdrawn, the wire was always in the shear layer. Hence, minor errors in resetting were readily noted as velocity changes.

The mean velocity ($\underline{u}$) was read directly from the anemometer's DC meter. The RMS value of the turbulence ($\underline{u}_T$) was read directly from the RMS meter. Both $\underline{u}$ and $\underline{u}_T$, as recorded, were vector summations of velocity components in the x and y directions. Figure 9 below illustrates the coordinates and components of $\underline{u}$. In the figure, the components of $\underline{u}_T$ may be obtained by direct addition of the r-subscript to the u's.

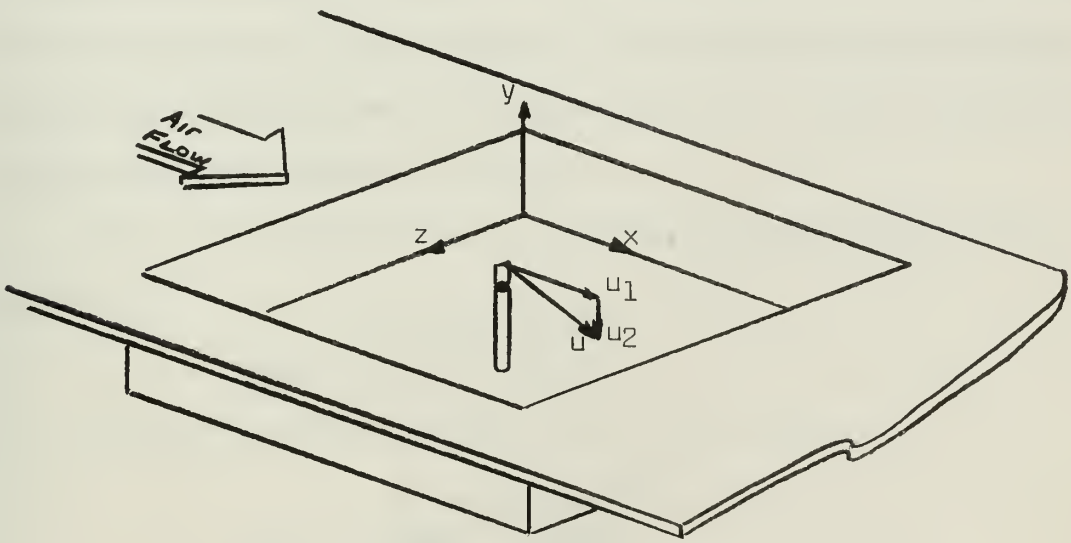

Figure 9 Coordinate Orientation and Velocity Components

Meter readings were visually averaged, using up to twenty needle swings per reading where fluctuations warranted.

Turbulence waveforms were observed by direct observation of the anemometer output on an oscilloscope. Pictures were taken off the scope with the vertical sensitivity set at 50 millivolts per centimeter and horizontal sensitivity at 2 milliseconds per centimeter.

5. Uncertainties and Sources of Error

Uncertainties and maximum errors for the various measured quantities and instruments used for this investigation were assigned as follows:

dynamic head (q)	± 1.0%
air density (ρ)	± 2.0%
cavity dimensions	± 0.01 inch
coordinate measurements	± 0.02 inch
anemometer meter needle swing	± 0.02 volts
RMS meter needle swing	± 0.005 volts
mean velocity change/0.01 inch change in probe location	± 0.015 volts
turbulence change/0.01 inch change in probe location	± 0.0015 volts
anemometer meter accuracy	± 0.005 volts
RMS meter accuracy	± 0.002 volts

From the above assigned limits of accuracy, uncertainties for the various controlled quantities were computed following standard techniques of computing the uncertainty as the square root of the sum of the squares of the component uncertainties. Component uncertainties were computed as the limit of accuracy divided by the value at the limit.

Hence, the uncertainty in the free stream velocity was computed as

$$\omega_U = \sqrt{(\omega_q)^2 + (\omega_\rho)^2}$$

Similarly for the uncertainty in x/L, etc.

$$\omega_{x/L} = \sqrt{\left(\frac{\Delta x}{x}\right)^2 + \left(\frac{\Delta L}{L}\right)^2}$$

Uncertainty calculations for the controlled quantities yielded the values following.

a.	Free stream velocity (U)	± 2.24%
b.	Hot wire locations: (x/L)	± 2.51%
	(z/W)	± 1.11%
	(y)	± 0.02 inch
c.	Velocity ratios: ($\underline{u}$)	± 6.10%
	($\underline{u}_r$)	± 7.70%

6. Results

At the end of this report velocity mappings from the data in Appendix I are included as Figures 10 through 15. The mappings consist of compilations of the data recorded within the x-y plane at z/W equal to 0.5 and within the y-z plane at x/L equal to 0.5 for the three inch deep cavity, and within the x-y plane at z/W equal to 0.5 only for the four inch deep cavity. The contour lines enclose areas of the plane where the velocity ratios had, as an upper bound, the number appearing on the contour. Where data was insufficient to force closure, the lines were extended up or down by dashed lines to indicate whether the enclosed data was above or below the contour.

The mean velocity ratios versus x/L at y/D and z/W equal to 0.5 are presented in Figure 16. This data is compared to corresponding estimated values of Roshko (9) at a similar relative location.

Lastly, pictures showing turbulence waveforms are included as Figures 17 and 18.

7. Discussion of Results

Nowhere in the literature encountered on cavity resonance are there presented either analytical solutions or experimental findings for the vortex velocity profiles, so that reliability of the collected data was entirely dependent on the following:

a. repeatability of data

b. comparison of the data with the estimated profile presented by Roshko (9)

c. comparison of the vortex velocity contours with results expected from inferences in the literature

The repeatability of the data was observed by accident when run number 38 was found to have been taken at the same points as run number 37. Forty-nine percent of the data points for runs 37 and 38 compared exactly, with the maximum separation of data points being 0.01 for $\underline{u}$ and 0.005 for $\underline{u}_r$, within the ranges defined in chapter 5. It should be noted, however, that the time separation between data points was only about forty-five minutes and involved no shut-downs or start-ups of the equipment. Hence the data repeatability cannot be categorized as confirmed. Additional repeat runs were not possible due to failure of the tunnel drive system just prior to completion of run number 40.

The comparison of results with Roshko's estimated profile in Figure 16 reveals data - estimation separation less than or equal to $\underline{u}$ of 0.02 within the range of x/L equal to 0.02 through 0.6. Above x/L equal to 0.6, the separation increased to 0.04 at x/L equal to 0.75 and to 0.05 at x/L equal to 0.8. This

result is tentatively attributed to the effects of the cavity side walls which were not included in Roshko's work and which are observed in Figures 10 and 11 to contribute significantly to the center section contours. This effect is believed to result from the interference of pressure disturbances meeting at the vortex center section. Because Roshko's apparatus might have more closely approximated a two dimensional cavity, having a W/L ratio of 8.5 vice the 3.0 ratio used in this investigation, it is quite likely that end effects were negligible in the prior work.

The appearance of definite vortex velocity profiles, particularly apparent in Figure 14, is, in minimal manner, an indication of reliability of the collected results. The reader is cautioned, however, that the velocity contours do not necessarily represent streamlines, since the hot-wire does not provide velocity direction information.

As was predicted by Roshko, Dunham (9, 2), and others, the vortex in the cavity having the higher D/L ratio shows much better definition, with core $\underline{u}$'s and $\underline{u}_r$'s down to 0.015 compared with minimum $\underline{u}$'s and $\underline{u}_r$'s of 0.09 and 0.035 respectively in the shallower cavity.

The appearance of two vortex cores in the three inch deep cavity was not predicted, but agrees with the general observation that stability and definition vary directly with the D/L ratio.

The consistent velocity disturbance observed at the bottom of the cavity is attributed to the presence of the discontinuity

which permitted entry of the probe into the cavity. While maintained at as small an opening as possible, the discontinuity in effect created an outlet from the main cavity into a second cavity.

A decided three-dimensional dependence was observed as mentioned above. The possibility of such dependence was postulated by Dunham (2), who noted that effects of the cavity sides had been neglected in all prior investigations. As a consequence of tunnel failure, data was collected in the y-z plane for only the three inch deep cavity and therefore no geometric comparisons were possible.

The tendency of the vortices to assume squared shapes outside the roughly circular core is attributed to the viscous shear effects originating at the cavity walls.

Two additional features of the vortices are granted singular importance. First, the presence of a strong turbulent zone immediately above and upstream of the vortex core in the four inch deep cavity is not an expected result. This, however, may be an advanced phase of the interface between the two cores observed in the three inch deep cavity. If this is the case, it would be expected that this turbulent region would move up into the shear layer and out of the cavity at higher L/D ratios. Further investigation of this area is needed.

Lastly, inasmuch as periodic fluctuations had been observed at the walls and in the shear layer, it was anticipated that the cavity turbulence would also contain well defined frequencies, from which comparisons of turbulence, mean velocity, and core definition might be related to Strouhal numbers. However, as

can be seen in Figures 17 and 18, no such periodicity of the turbulence was found. It is possible that periodic regimes might be recognized by use of a frequency spectrum analyzer or a tape data retrieval system and computer processing. Such equipment was not available for this program. It may also be speculated that some geometric or boundary layer conditions conducive to periodic vortex formation were not met in the present arrangement. This would dictate that an analysis of the requirements for observing periodicity within the vortex should be made, but it is not within the scope of this investigation to do so. Such an analysis could draw from that of Dunham (2) for conditions required to observe periodicity in the shear layer vortices.

8. Conclusions

1. The constant temperature hot wire anemometer can be used to observe velocity profiles in a flow induced standing vortex in an open cavity.

2. Strong turbulence is introduced into the boundary layer by the presence of an open cavity, and this turbulence extends throughout the standing vortex induced in the cavity, though to a lesser degree.

3. Strong three-dimensional effects exist in the captive vortex at W/L ratios as high as 3.0, and are not confined to the ends of the vortex, but are reflected to the midsection as well.

4. Vortex definition is strongly dependent on D/L ratios, with a D/L ratio of 1.0 yielding a single vortex core.

5. Turbulence within the vortex does not exhibit strong periodicity at low Mach numbers.

9. Recommendations for Future Study

The test apparatus used for this investigation provides sufficient flexibility so that some or all of the following proposals can be coupled to the present or a slightly modified system.

More extensive probing of the test cavities is needed to provide truly definitive data on the existing vortices. For the same reason, more geometries should be investigated. Both L/D and L/W should be varied and results compared. As mentioned in the discussion of results, observation of the two-core interface to determine whether or not it degenerates into the high turbulence region could be a significant portion of this effort.

Some steps should be taken to reduce or control the boundary layer thickness upstream of the cavity including a) relocation of the cavity such that its mouth would be at the tunnel centerline vice the tunnel floor and b) perforation of the upstream surface, thereby allowing the boundary layer to be controlled by use of a vacuum system.

An effort to determine if fluid is truly isolated in the vortex or if there is transport in and out of the vortex should be considered.

Cross-correlation techniques, use of a frequency spectrum analyzer and/or use of a tape data retrieval system with computer processing should be coupled with any of the preceding recommendations and would additionally be necessary for investigations of the effects of vortex fluctuations on acoustic outputs or of the possibility of the existence of additional stable

states within the cavity and regimes where more than one state may be found.

The ability to develop a free standing vortex system, the control of its form by judicious use of either geometric or boundary layer control changes, and the introduction of controlled disturbances such as acoustic waves makes possible the continuation of this problem in the general field of vortex stability. It is quite possible that a logical sequence of experiments could serve as a useful adjunct to work of other experimenters in the area of bluff body separated flow, with the end result of developing a clearer understanding of a three-dimensional problem that has puzzled investigators for over a hundred years. The recognition of separated flow being three-dimensional in character within the past twenty years has been a significant step, and it now remains to apply recently developed experimental tools in order to define the problem further.

BIBLIOGRAPHY

1. Blokhintsev, D. I., "Excitation of Resonance by Air Flow," SLA Translation Pool No. 270 (ONR) from ZATF Vol. 15, pp 63-70 (1945).

2. Dunham, W. H., "Flow Induced Cavity Resonance in Viscous Compressible and Incompressible Fluids," Fourth Symposium on Naval Hydrodynamics, ONR ACR-92 pp 1057-1081 (1962).

3. Fail, R., Owen, R. B., and Eyre, R. C. W., "Low Speed Tunnel Tests on the Flow in Bomb Bays and Its Effect on Drag and Vibration," A.R.C. 17412. (May, 1954).

4. Harrington, M. C. and Dunham, W. H., "Studies of the Mechanism for Flow-Induced Cavity Resonances," Journal Acoustical Society of America, Vol. 32, p 921 (July 1960).

5. Hinze, J. O., Turbulence. New York; McGraw-Hill Book Company, Inc. (1959).

6. Krishnamurty, K., "Acoustic Radiation from Two-dimensional Rectangular Cutouts in Aerodynamic Surfaces," NACA TN 3487 (1955).

7. Liepmann, H. W., Laufer, J., and Liepmann, Kate, "On the Spectrum of Isotropic Turbulence," NACA TN 2473 (1951).

8. Roshko, Anatol, "On the Development of the Turbulent Wakes from Vortex Streets," NACA TN 2913 (1953).

9. Roshko, Anatol, "Some Measurements of Flow in a Rectangular Cutout," NACA TN 3488 (1955).

10. Rossiter, J. E., "Wind Tunnel Experiments on the Flow Over Rectangular Cavities at Subsonic and Transonic Speeds," ARC R and M No. 3438 (October, 1964).

11. Streeter, Victor L., Fluid Mechanics. New York; McGraw-Hill Book Company, Inc. (1962).

12. Tillman, W., "Additional Measurements of the Drag of Surface Irregularities in Turbulent Boundary Layers," NACA TN 1299 (January, 1951).

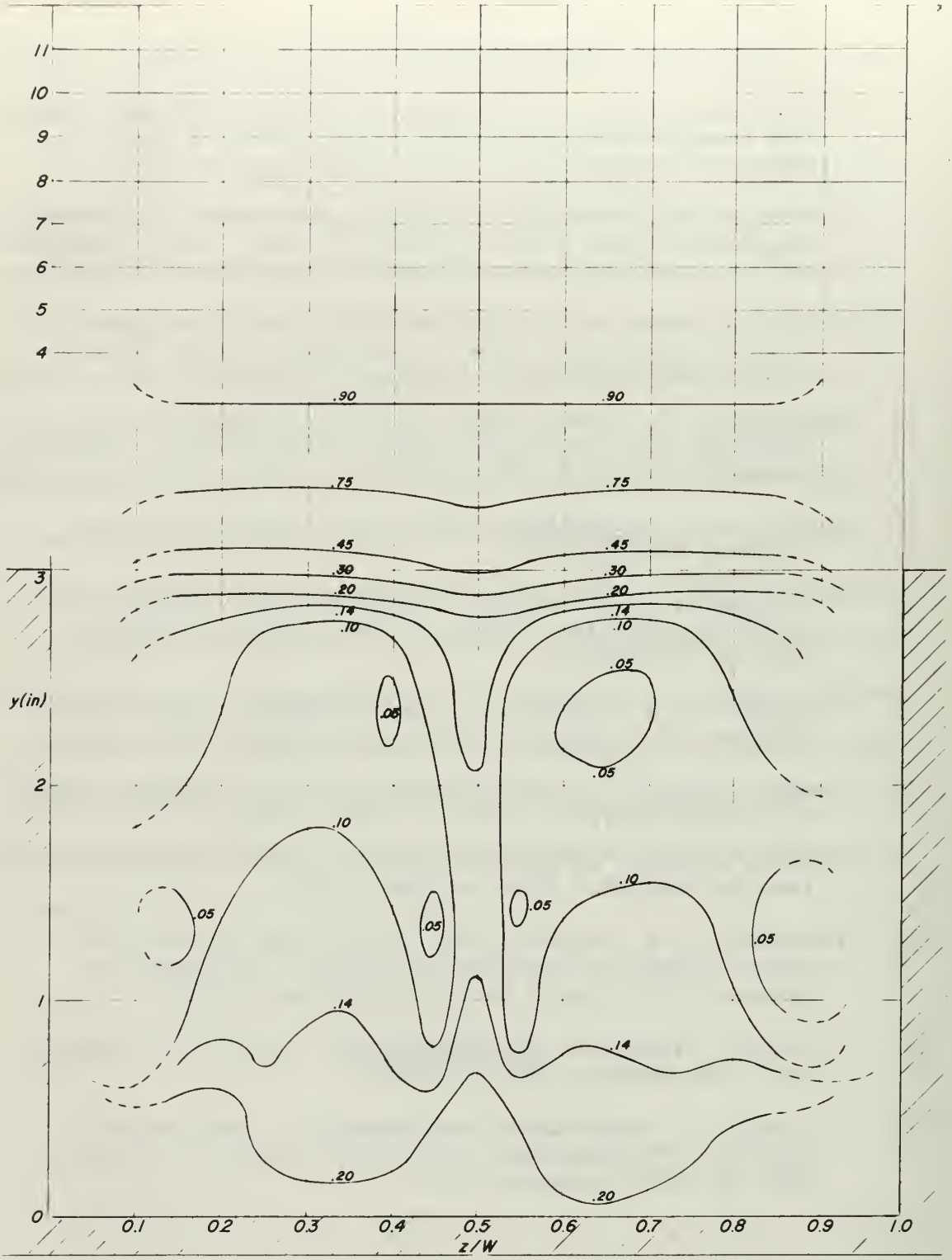

FIGURE 10 MEAN VELOCITY CONTOURS IN SPANWISE DIRECTION, $D/L = 0.75$, $x/L = 0.5$

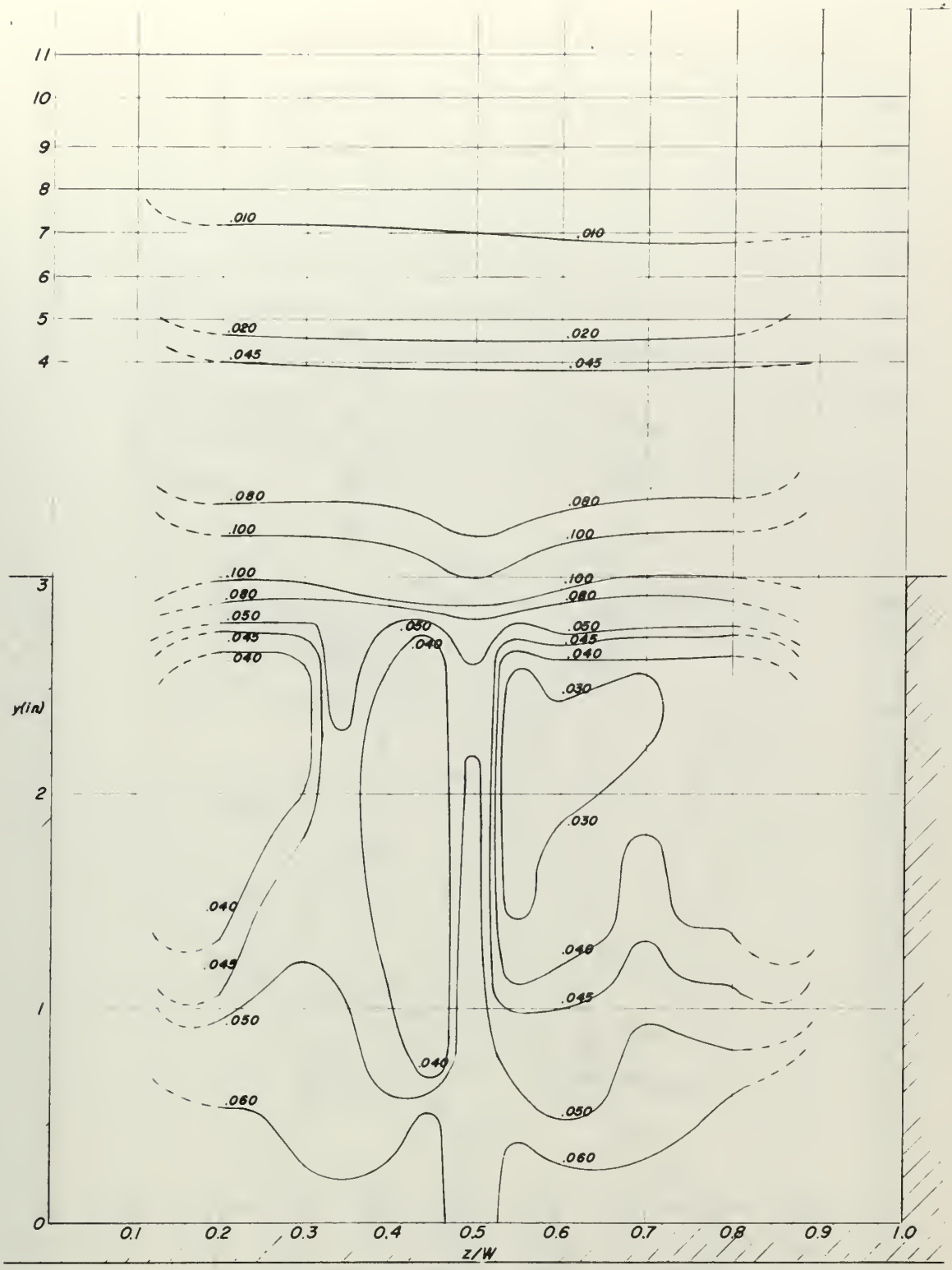

FIGURE 11 UNSTEADY VELOCITY CONTOURS IN SPANWISE DIRECTION, D/L = 0.75, x/L = 0.5

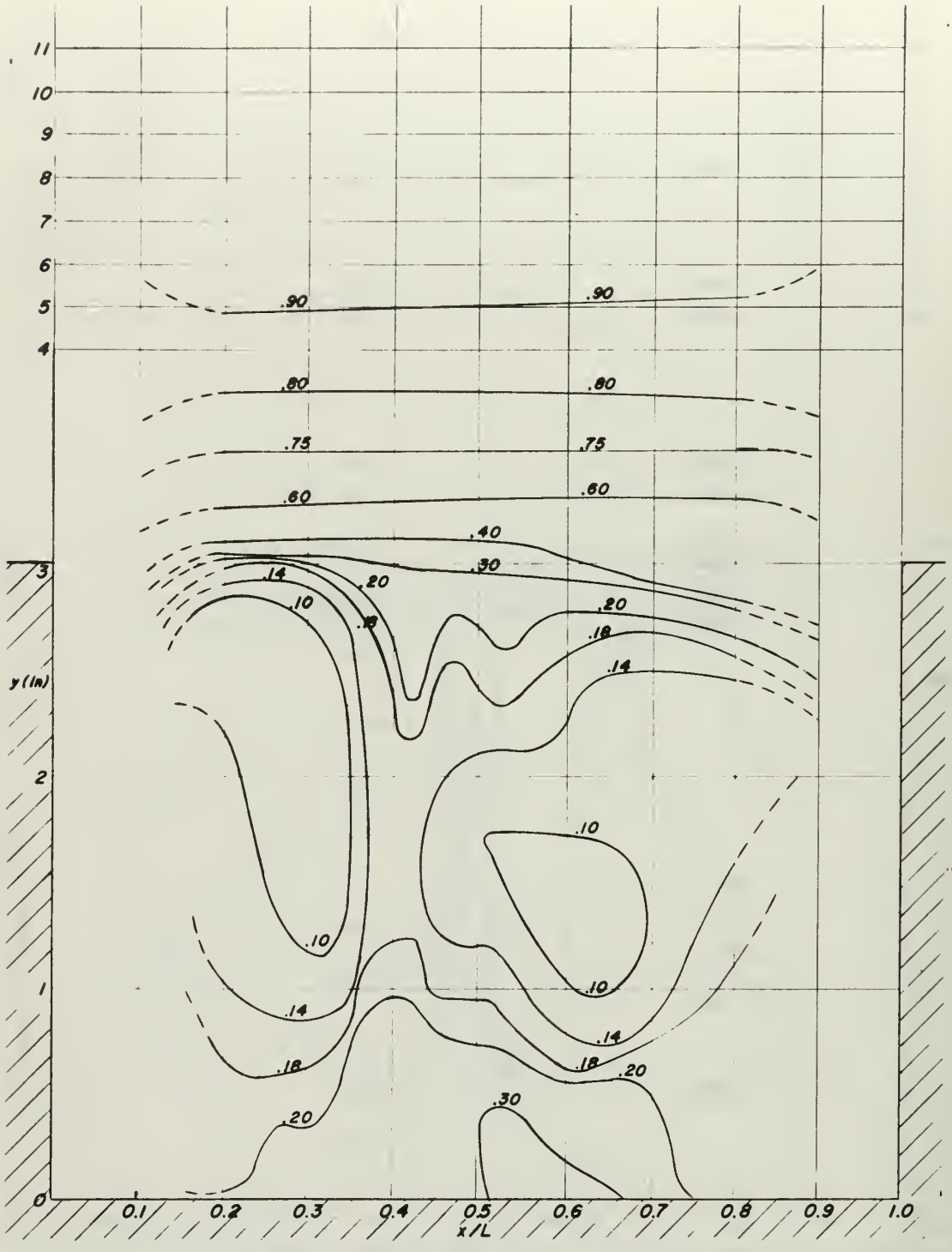

FIGURE 12 MEAN VELOCITY CONTOURS IN CHORDWISE DIRECTION, D/L = 0.75, z/W = 0.5

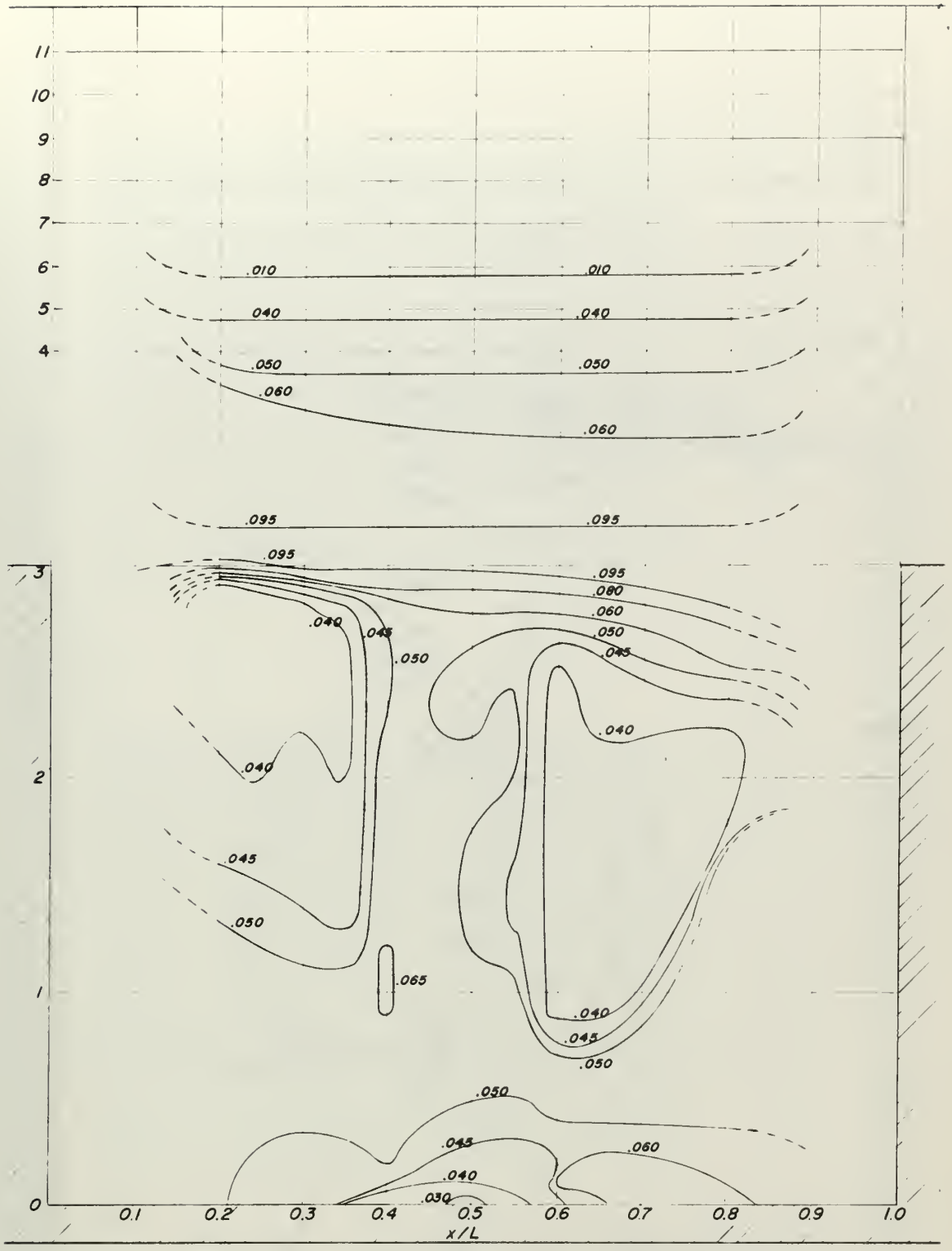

FIGURE 13 UNSTEADY VELOCITY CONTOURS IN CHORDWISE DIRECTION D/L = 0.75 z/W = 0.5

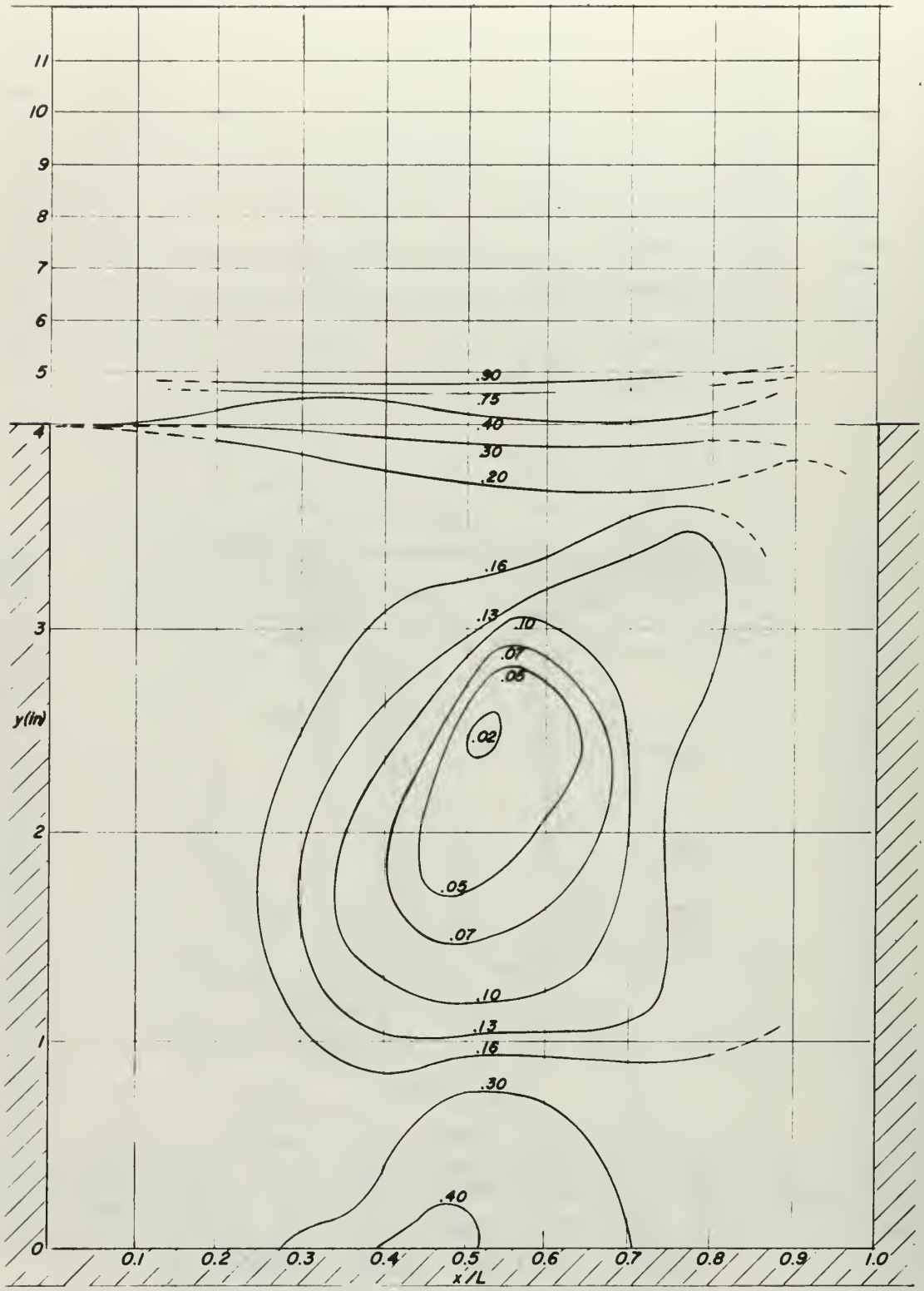

FIGURE 14 MEAN VELOCITY CONTOURS IN CHORDWISE DIRECTION, D/L = 1.0, z/W = 0.5

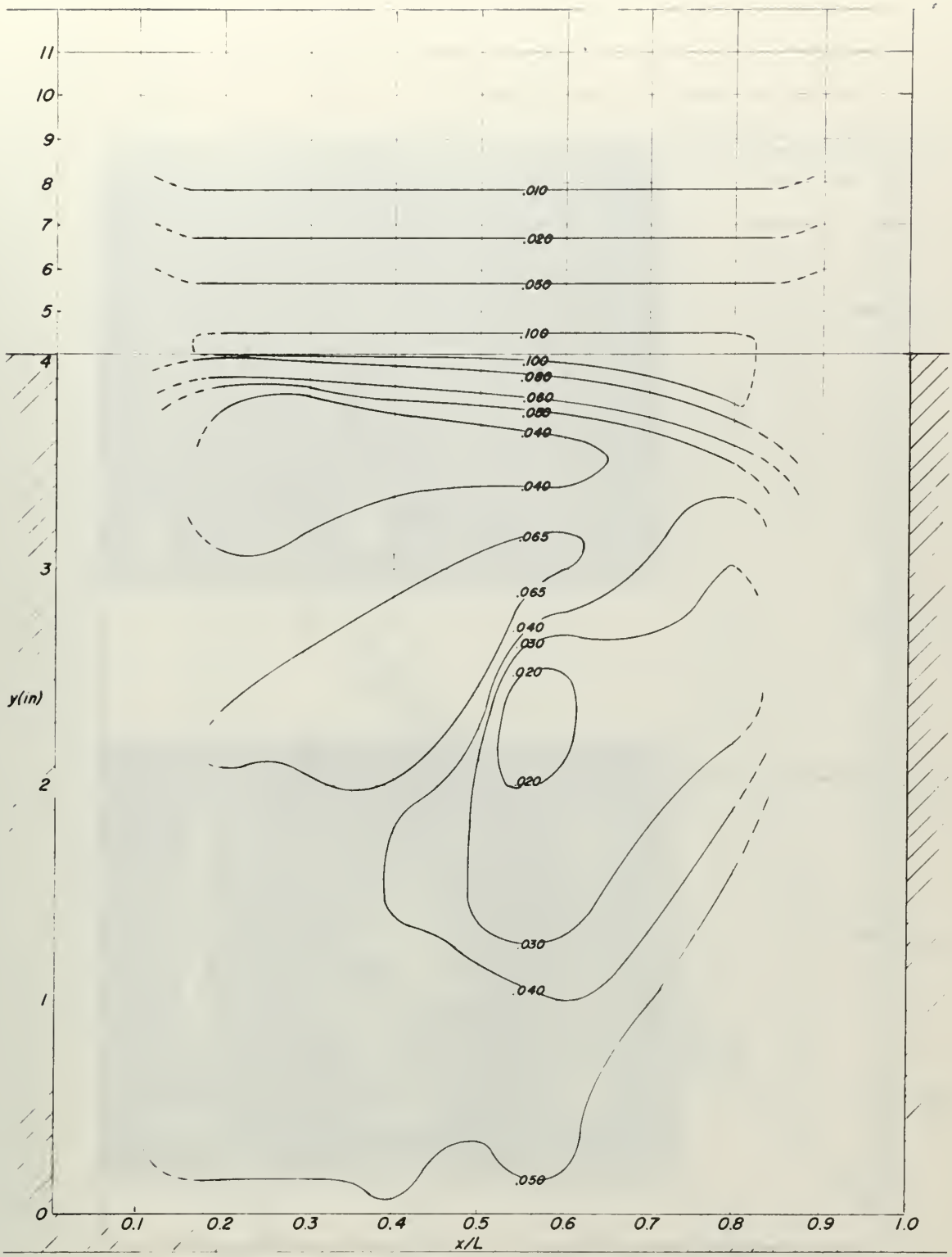

FIGURE 15 UNSTEADY VELOCITY CONTOUR IN CHORDWISE DIRECTION, D/L = 1.0, z/W = 0.5

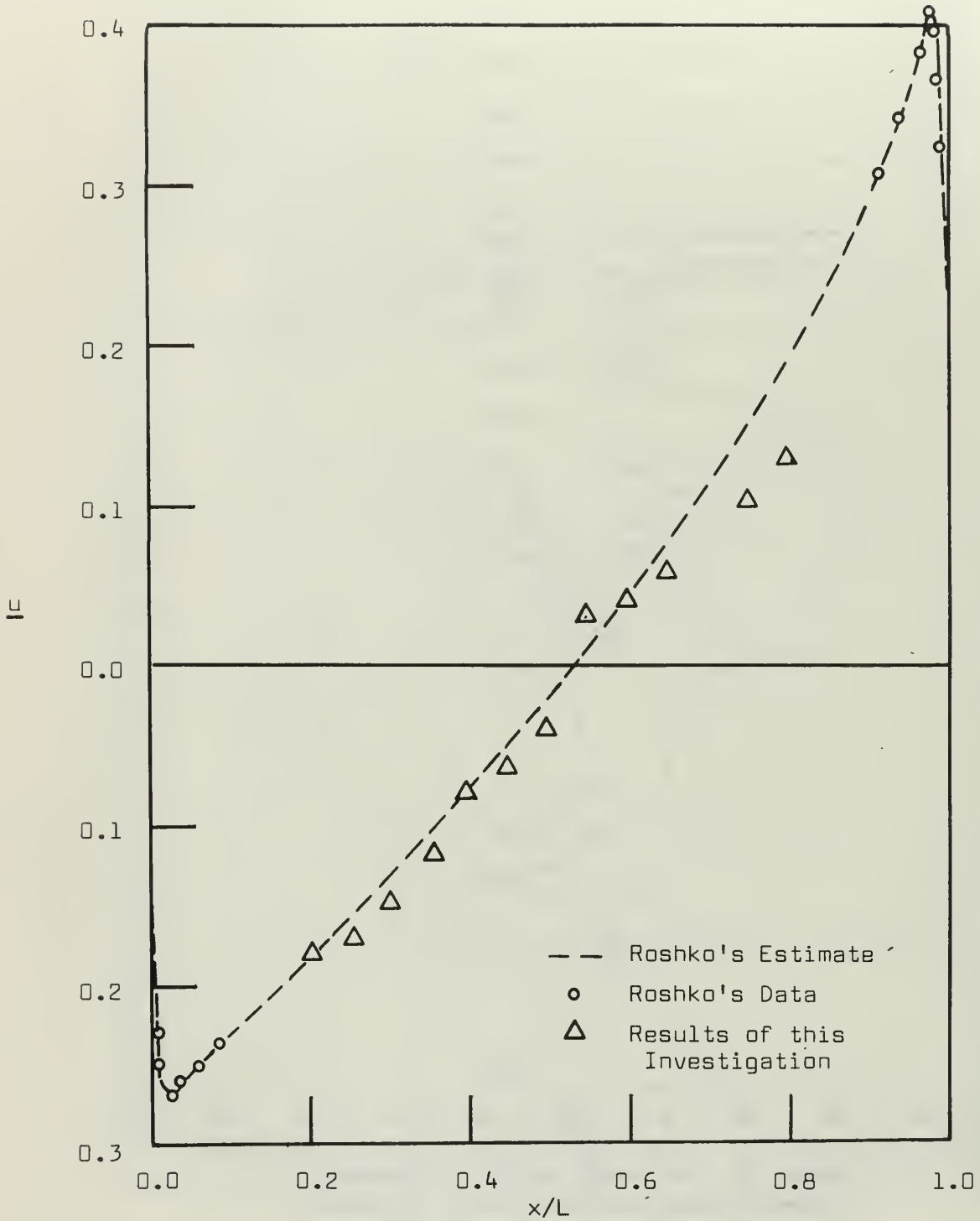

Figure 16 - $\underline{u}$ versus x/L for y/D and z/W=0.5, D/L=1.0

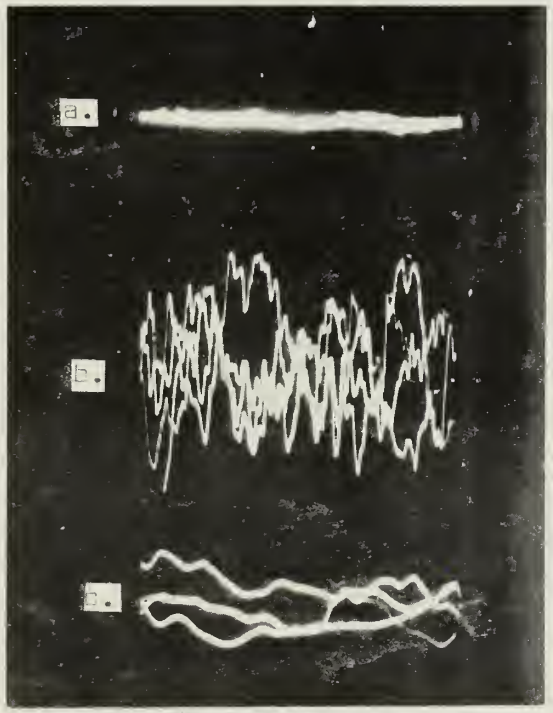

a. y/D=2.3
b. y/D=1.5
c. y/D=1.0

Figure 1E - Turbulence Waveform, y/D=2.75

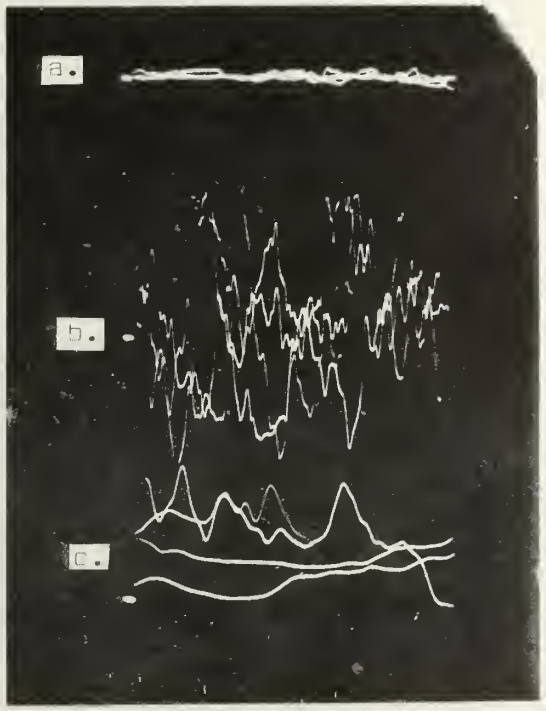

a. y/D=2.5
b. y/D=1.5
c. y/D=1.0

Figure 1F - Turbulence Waveform, y/D=3.0

APPENDIX I

Run Data

Run 1

x/L = 0.5 T = 70°F

z/W = 0.5 q = 6.67 lbs/ft^2

D/L = 0.75

y (in	$\frac{u}{}$	$\frac{u}{}_T$	y (in)	$\frac{u}{}$	$\frac{u}{}_T$
0.0	.05	.027	2.5	.16	.046
0.1	.22	.044	2.6	.17	.047
0.2	.22	.045	2.7	.18	.055
0.3	.24	.048	2.8	.23	.075
0.4	.23	.05	2.9	.33	.090
0.5	.23	.055	3.0	.45	.100
0.6	.21	.055	3.1	.60	.095
0.7	.20	.059	3.2	.70	.080
0.8	.19	.056	3.3	.76	.067
0.9	.18	.055	3.4	.79	.065
1.0	.16	.055	3.5	.82	.06
1.1	.15	.055	3.6	.86	.055
1.2	.14	.05	3.7	.88	.055
1.3	.12	.052	3.8	.89	.05
1.4	.11	.05	3.9	.89	.04
1.5	.11	.05	4.0	.90	.040
1.6	.11	.052	6.0	.98	.012
1.7	.11	.052	6.0	.98	.012
1.8	.12	.058	7.0	.99	.011
1.9	.12	.055	8.0	1.0	.009
2.0	.13	.055	9.0	1.0	.007
2.1	.14	.053	10.0	1.0	.006
2.2	.15	.05			
2.3	.16	.047			
2.4	.16	.045			

Run 2

x/L = 0.5 T = 74°F

z/W = 0.15 q = 6.67 lbs/ft^2

D/L = 0.75

y (in	$\frac{u}{}$	$\frac{u}{}_r$	y (in)	$\frac{u}{}$	$\frac{u}{}_r$
0.0	.31	.060	2.5	.13	.035
0.1	.25	.075	2.6	.14	.035
0.2	.22	.068	2.7	.14	.040
0.3	.23	.072	2.8	.19	.060
0.4	.22	.062	2.9	.29	.090
0.5	.19	.057	3.0	.43	.105
0.6	.15	.055	3.1	.58	.100
0.7	.12	.050	3.2	.68	.088
0.8	.10	.045	3.3	.76	.070
0.9	.08	.040	3.4	.80	.065
1.0	.07	.037	3.5	.82	.065
1.1	.06	.036	3.6	.85	.065
1.2	.05	.037	3.7	.88	.060
1.3	.04	.035	3.8	.90	.050
1.4	.05	.035	3.9	.93	.050
1.5	.05	.038	4.0	.93	.050
1.6	.06	.041	5.0	.97	.020
1.7	.08	.041	6.0	.98	.013
1.8	.09	.042	7.0	.99	.017
1.9	.10	.042	8.0	.99	.009
2.0	.11	.038	9.0	1.0	.008
2.1	.12	.038	10.0	1.0	.008
2.2	.12	.036			
2.3	.13	.035			
2.4	.13	.035			

Run 3

x/L = 0.5

z/W = 0.20

D/L = 0.75

T = 75°F

q = 6.67 lbs/ft^2

y (in)	$\frac{u}{}$	$\frac{u}{}_r$	y (in)	$\frac{u}{}$	$\frac{u}{}_r$
0.0	.31	.050	2.5	.12	.037
0.1	.27	.075	2.6	.12	.035
0.2	.21	.070	2.7	.14	.038
0.3	.22	.074	2.8	.17	.050
0.4	.23	.065	2.9	.24	.085
0.5	.21	.059	3.0	.39	.100
0.6	.18	.057	3.1	.52	.105
0.7	.17	.053	3.2	.65	.095
0.8	.15	.050	3.3	.75	.075
0.9	.14	.050	3.4	.79	.067
1.0	.13	.045	3.5	.82	.065
1.1	.12	.043	3.6	.85	.060
1.2	.11	.040	3.7	.85	.055
1.3	.10	.039	3.8	.89	.055
1.4	.09	.038	3.9	.91	.055
1.5	.09	.039	4.0	.93	.045
1.6	.09	.039	5.0	.98	.017
1.7	.08	.041	6.0	.99	.010
1.8	.07	.041	7.0	1.0	.010
1.9	.08	.043	8.0	1.0	.009
2.0	.08	.042	9.0	1.0	.007
2.1	.09	.042	10.0	1.0	.007
2.2	.10	.040			
2.3	.11	.040			
2.4	.11	.037			

Run 4

x/L = 0.5 T = 78°F

z/W = 0.25 q = 6.67 lbs/ft^2

D/L = 0.75

y (in)	$\underline{u}$	$\underline{u}_r$	y (in)	$\underline{u}$	$\underline{u}_r$
0.0	.32	.055	2.5	.08	.038
0.1	.25	.085	2.6	.09	.038
0.2	.19	.075	2.7	.10	.043
0.3	.20	.070	2.8	.14	.055
0.4	.20	.062	2.9	.22	.082
0.5	.18	.060	3.0	.36	.105
0.6	.16	.055	3.1	.51	.110
0.7	.14	.052	3.2	.65	.100
0.8	.13	.050	3.3	.74	.080
0.9	.13	.050	3.4	.79	.075
1.0	.13	.050	3.5	.82	.065
1.1	.13	.045	3.6	.85	.060
1.2	.13	.045	3.7	.88	.060
1.3	.125	.043	3.8	.90	.050
1.4	.12	.045	3.9	.92	.045
1.5	.12	.040	4.0	.95	.048
1.6	.11	.040	5.0	.985	.019
1.7	.10	.038	6.0	1.0	.012
1.8	.10	.037	7.0	1.0	.010
1.9	.09	.036	8.0	1.0	.009
2.0	.08	.035	9.0	1.0	.008
2.1	.075	.037	10.0	1.0	.008
2.2	.08	.037			
2.3	.08	.038			
2.4	.08	.038			

Run 5

x/L = 0.5 T = 72°F

z/W = 0.30 q = 6.67 lbs/ft^2

D/L = 0.75

y (in)	$\frac{u}{}$	$\frac{u}{}_T$	y (in)	$\frac{u}{}$	$\frac{u}{}_T$
0.0	.26	.040	2.5	.08	.038
0.1	.25	.058	2.6	.09	.038
0.2	.21	.058	2.7	.10	.040
0.3	.19	.057	2.8	.14	.055
0.4	.18	.057	2.9	.25	.090
0.5	.17	.055	3.0	.38	.107
0.6	.16	.055	3.1	.53	.105
0.7	.16	.055	3.2	.65	.095
0.8	.15	.055	3.3	.77	.065
0.9	.14	.055	3.4	.77	.065
1.0	.14	.050	3.5	.82	.065
1.1	.13	.050	3.6	.84	.055
1.2	.13	.048	3.7	.87	.055
1.3	.13	.047	3.8	.88	.050
1.4	.12	.045	3.9	.89	.045
1.5	.12	.046	4.0	.91	.040
1.6	.11	.045	5.0	.96	.015
1.7	.11	.044	6.0	.98	.010
1.8	.10	.042	7.0	.99	.010
1.9	.09	.040	8.0	.99	.007
2.0	.09	.038	9.0	1.0	.007
2.1	.08	.037	10.0	1.0	.008
2.2	.07	.037			
2.3	.07	.037			
2.4	.07	.038			

Run 6

x/L = 0.5 T = 76°F

z/W = 0.35 q = 6.67 lbs/ft^2

D/L = 0.75

y (in)	$\frac{u}{}$	$\frac{u}{}_r$	y (in)	$\frac{u}{}$	$\frac{u}{}_r$
0.0	.26	.070	2.5	.085	.050
0.1	.23	.060	2.6	.09	.050
0.2	.175	.045	2.7	.10	.050
0.3	.18	.047	2.8	.12	.060
0.4	.185	.045	2.9	.20	.085
0.5	.19	.045	3.0	.32	.105
0.6	.18	.050	3.1	.50	.110
0.7	.17	.050	3.2	.63	.100
0.8	.16	.050	3.3	.71	.080
0.9	.15	.050	3.4	.76	.075
1.0	.14	.050	3.5	.80	.065
1.1	.135	.050	3.6	.84	.060
1.2	.13	.045	3.7	.86	.055
1.3	.13	.045	3.8	.88	.050
1.4	.12	.045	3.9	.89	.048
1.5	.115	.045	4.0	.92	.040
1.6	.11	.045	5.0	.96	.020
1.7	.105	.045	6.0	.98	.011
1.8	.10	.045	7.0	.99	.010
1.9	.10	.045	8.0	.99	.009
2.0	.09	.045	9.	1.0	.007
2.1	.085	.045	10.0	1.0	.007
2.2	.08	.045			
2.3	.08	.050			
2.4	.085	.050			

Run 7

x/L = 0.5 T = 78°F

z/W = 0.40 q = 6.67 lbs/ft^2

D/L = 0.75

y (in)	$\frac{u}{}$	$\frac{u}{}_r$	y (in)	$\frac{u}{}$	$\frac{u}{}_r$
0.0	.26	.070	2.5	.05	.040
0.1	.21	.085	2.6	.07	.045
0.2	.18	.065	2.7	.08	.045
0.3	.20	.055	2.8	.13	.065
0.4	.19	.050	2.9	.22	.100
0.5	.17	.050	3.0	.37	.115
0.6	.15	.045	3.1	.53	.110
0.7	.13	.045	3.2	.65	.095
0.8	.13	.045	3.3	.74	.080
0.9	.125	.045	3.4	.80	.070
1.0	.115	.045	3.5	.83	.065
1.1	.11	.045	3.6	.85	.065
1.2	.11	.040	3.7	.89	.065
1.3	.110	.040	3.8	.90	.050
1.4	.100	.040	3.9	.92	.045
1.5	.095	.040	4.0	.95	.045
1.6	.09	.038	5.0	.99	.017
1.7	.09	.038	6.0	1.0	.012
1.8	.085	.038	7.0	1.0	.010
1.9	.075	.035	8.0	1.0	.009
2.0	.065	.035	9.0	1.0	.007
2.1	.055	.035	10.0	1.0	.077
2.2	.05	.035			
2.3	.05	.035			
2.4	.05	.040			

Run 8

x/L = 0.5 T = 80°f

z/W = 0.45 q = 6.67 lbs/ft^2

D/L = 0.75

y (in)	$\frac{u}{}$	$\frac{u}{}_r$	y (in)	$\frac{u}{}$	$\frac{u}{}_r$
0.0	.37	.055	2.5	.125	.035
0.1	.32	.075	2.6	.13	.035
0.2	.23	.080	2.7	.14	.035
0.3	.25	.080	2.8	.17	.060
0.4	.23	.070	2.9	.25	.100
0.5	.17	.060	3.0	.40	.110
0.6	.14	.050	3.1	.55	.110
0.7	.11	.040	3.2	.68	.090
0.8	.085	.035	3.3	.75	.075
0.9	.07	.035	3.4	.80	.070
1.0	.06	.030	3.5	.83	.070
1.1	.055	.030	3.6	.86	.065
1.2	.05	.030	3.7	.89	.060
1.3	.04	.025	3.8	.91	.055
1.4	.04	.030	3.9	.92	.045
1.5	.045	.035	4.0	.94	.045
1.6	.055	.035	5.0	.985	.017
1.7	.065	.035	6.0	1.0	.011
1.8	.07	.040	7.0	1.0	.011
1.9	.085	.035	8.0	1.0	.008
2.0	.095	.035	9.0	1.0	.006
2.1	.10	.035	10.0	1.0	.006
2.2	.105	.032			
2.3	.11	.033			
2.4	.12	.033			

Run 9

x/L = 0.5 T = 78°F

z/W = 0.55 q = 6.67 lbs/ft^2

D/L = 0.75

y (in)	$\frac{u}{}$	$\frac{u}{}_T$	y (in)	$\frac{u}{}$	$\frac{u}{}_T$
0.0	.27	.080	2.5	.07	.030
0.1	.21	.065	2.6	.08	.035
0.2	.20	.065	2.7	.10	.040
0.3	.23	.065	2.8	.18	.050
0.4	.19	.050	2.9	.24	.080
0.5	.15	.050	3.0	.37	.100
0.6	.15	.050	3.1	.50	.105
0.7	.095	.040	3.2	.62	.090
0.8	.08	.035	3.3	.70	.075
0.9	.10	.045	3.4	.76	.065
1.0	.095	.040	3.5	.79	.065
1.1	.085	.035	3.6	.81	.060
1.2	.08	.035	3.7	.84	.055
1.3	.07	.035	3.8	.87	.050
1.4	.045	.030	3.9	.88	.045
1.5	.065	.030	4.0	.92	.045
1.6	.06	.030	6.0	.98	.013
1.7	.05	.030	6.0	.99	.010
1.8	.07	.030	7.0	.995	.008
1.9	.09	.030	8.0	1.0	.008
2.0	.09	.030	9.0	1.0	.006
2.1	.05	.030	10.0	1.0	.006
2.2	.045	.030			
2.3	.11	.030			
2.4	.105	.030			

Run 10

x/L = 0.5 T = 72°F

z/W = 0.60 q = 6.67 lbs/ft^2

D/L = 0.75

y (in)	$\frac{u}{}$	$\frac{u}{}_T$	y (in)	$\frac{u}{}$	$\frac{u}{}_T$
0.0	.23	.050	2.5	.065	.035
0.1	.175	.055	2.6	.08	.040
0.2	.190	.060	2.7	.11	.050
0.3	.195	.090	2.8	.17	.070
0.4	.19	.045	2.9	.28	.095
0.5	.17	.045	3.0	.42	.109
0.6	.16	.045	3.1	.57	.100
0.7	.15	.045	3.2	.69	.085
0.8	.14	.045	3.3	.76	.070
0.9	.13	.045	3.4	.81	.065
1.0	.125	.040	3.5	.83	.060
1.1	.12	.040	3.6	.86	.060
1.2	.11	.035	4.7	.90	.050
1.3	.11	.035	3.8	.90	.050
1.4	.105	.035	3.9	.92	.050
1.5	.10	.035	4.0	.94	.040
1.6	.09	.035	5.0	.975	.017
1.7	.085	.035	6.0	.99	.009
1.8	.075	.035	7.0	.995	.009
1.9	.07	.030	8.0	1.0	.008
2.0	.06	.030	9.0	1.0	.006
2.1	.055	.030	10.0	1.0	.006
2.2	.05	.030			
2.3	.05	.030			
2.4	.055	.035			

Run 11

x/L = 0.5 T = 72°F

z/W = 0.65 q = 6.67 lbs/ft^2

D/L = 0.75

y (in)	$\frac{u}{}$	$\frac{u}{}_T$	y (in)	$\frac{u}{}$	$\frac{u}{}_T$
0.0	.26	.055	2.5	.05	.035
0.1	.20	.070	2.6	.06	.035
0.2	.17	.065	2.7	.08	.040
0.3	.20	.060	2.8	.12	.055
0.4	.20	.048	2.9	.21	.080
0.5	.175	.045	3.0	.34	.105
0.6	.16	.045	3.1	.49	.110
0.7	.15	.045	3.2	.64	.095
0.8	.14	.045	3.3	.73	.080
0.9	.125	.045	3.4	.78	.070
1.0	.12	.045	3.5	.82	.065
1.1	.115	.040	3.6	.85	.065
1.2	.11	.040	3.7	.88	.055
1.3	.105	.035	3.8	.90	.055
1.4	.10	.035	3.9	.91	.045
1.5	.095	.035	4.0	.94	.040
1.6	.09	.035	5.0	.98	.015
1.7	.085	.035	6.0	.995	.010
1.8	.075	.033	7.0	1.0	.009
1.9	.065	.032	8.0	1.0	.008
2.0	.06	.030	9.0	1.0	.007
2.1	.05	.030	10.0	1.0	.006
2.2	.045	.030			
2.3	.045	.030			
2.4	.05	.030			

Run 12

x/L = 0.5 T = 76°F

z/W =0.70 q = 6.67 lbs/ft^2

D/L = 0.75

y (in)	$\frac{u}{}$	$\frac{u}{}_r$	y (in)	$\frac{u}{}$	$\frac{u}{}_r$
0.0	.28	.055	2.5	.045	.030
0.1	.21	.075	2.6	.06	.035
0.2	.16	.060	2.7	.075	.045
0.3	.175	.055	2.8	.11	.055
0.4	.17	.050	2.9	.21	.090
0.5	.16	.050	3.0	.34	.110
0.6	.15	.050	3.1	.49	.115
0.7	.14	.050	3.2	.64	.100
0.8	.135	.050	3.3	.73	.080
0.9	.13	.050	3.4	.79	.070
1.0	.125	.045	3.5	.82	.065
1.1	.125	.045	3.6	.86	.060
1.2	.12	.045	3.7	.88	.060
1.3	.115	.045	3.8	.90	.055
1.4	.11	.040	3.9	.92	.045
1.5	.105	.040	4.0	.94	.045
1.6	.10	.040	5.0	.985	.020
1.7	.095	.040	6.0	.995	.010
1.8	.085	.083	7.0	1.0	.009
1.9	.075	.035	8.0	1.0	.008
2.0	.07	.035	9.0	1.0	.007
2.1	.055	.035	10.0	1.0	.006
2.2	.045	.032			
2.3	.04	.030			
2.4	.04	.030			

Run 13

x/L = 0.5 T= 76°F

z/W = 0.75 q = 6.67 lbs/ft^2

D/L = 0.75

y (in)	$\frac{u}{}$	$\frac{u}{}_r$	y (in)	$\frac{u}{}$	$\frac{u}{}_r$
0.0	.29	.045	2.5	.06	.035
0.1	.23	.060	2.6	.07	.040
0.2	.17	.060	2.7	.09	.040
0.3	.19	.060	2.8	.125	.055
0.4	.175	.050	2.9	.21	.085
0.5	.16	.050	3.0	.34	.105
0.6	.15	.050	3.1	.50	.110
0.7	.14	.050	3.2	.63	.095
0.8	.13	.045	3.3	.72	.080
0.9	.13	.045	3.4	.77	.065
1.0	.125	.045	3.5	.81	.065
1.1	.125	.040	3.6	.84	.060
1.2	.12	.040	3.7	.86	.060
1.3	.12	.039	3.8	.89	.050
1.4	.12	.038	3.9	.90	.045
1.5	.115	.037	4.0	.925	.040
1.6	.105	.036	5.0	.975	.012
1.7	.10	.035	6.0	.985	.011
1.8	.085	.035	7.0	.99	.010
1.9	.08	.035	8.0	1.0	.009
2.0	.07	.035	9.0	1.0	.007
2.1	.065	.035	10.0	1.0	.006
2.2	.055	.035			
2.3	.055	.035			
2.4	.055	.035			

Run 14

x/L = 0.5 T = 79°F

z/W = 0.80 q = 6.67 lbs/ft^2

D/L = 0.75

y (in)	$\frac{u}{}$	$\frac{u}{}_r$	y (in)	$\frac{u}{}$	$\frac{u}{}_r$
0.0	.26	.070	2.5	.105	.037
0.1	.21	.070	2.6	.115	.037
0.2	.21	.070	2.7	.125	.040
0.3	.23	.065	2.8	.165	.055
0.4	.21	.060	2.9	.25	.085
0.5	.19	.060	3.0	.38	.105
0.6	.165	.060	3.1	.54	.105
0.7	.150	.055	3.2	.68	.090
0.8	.135	.050	3.3	.75	.080
0.9	.12	.045	3.4	.80	.070
1.0	.11	.045	3.5	.85	.070
1.1	.095	.045	3.6	.88	.065
1.2	.08	.040	3.7	.90	.055
1.3	.075	.040	3.8	.91	.055
1.4	.07	.035	3.9	.92	.045
1.5	.065	.035	4.0	.95	.040
1.6	.065	.035	5.0	.99	.015
1.7	.55	.035	6.0	1.0	.010
1.8	.055	.035	7.0	1.0	.009
1.9	.06	.035	8.0	1.0	.008
2.0	.06	.037	9.0	1.0	.007
2.1	.065	.037	10.0	1.0	.006
2.2	.07	.038			
2.3	.08	.038			
2.4	.085	.037			

Run 15

x/L = 0.5 T = 82°F

z/W = 0.85 q = 6.67 lbs/ft^2

D/L = 0.75

y (in)	$\frac{u}{}$	$\frac{u}{}_r$	y (in)	$\frac{u}{}$	$\frac{u}{}_r$
0.0	.28	.055	2.5	.125	.035
0.1	.22	.075	2.6	.13	.035
0.2	.24	.65	2.7	.15	.038
0.3	.24	.065	2.8	.18	.050
0.4	.20	.060	2.9	.25	.080
0.5	.16	.060	3.0	.38	.105
0.6	.135	.055	3.1	.53	.105
0.7	.11	.050	3.2	.66	.095
0.8	.08	.045	3.3	.74	.080
0.9	.055	.035	3.4	.79	.070
1.0	.045	.030	3.5	.83	.070
1.1	.035	.025	3.6	.85	.065
1.2	.03	.025	3.7	.87	.060
1.3	.03	.024	3.8	.90	.055
1.4	.035	.028	3.9	.92	.045
1.5	.04	.030	4.0	.95	.040
1.6	.05	.035	5.0	.985	.012
1.7	.065	.038	6.0	.995	.010
1.8	.08	.038	7.0	1.0	.008
1.9	.09	.038	8.0	1.0	.007
2.0	.10	.035	9.0	1.0	.006
2.1	.11	.035	10.0	1.0	.006
2.2	.12	.035			
2.3	.12	.035			
2.4	.12	.035			

Run 16

x/L = 0.55 T = 77°F

z/W = 0.5 q = 6.67 lbs/ft^2

D/L = 0.75

y (in)	$\frac{u}{}$	$\frac{u}{}_r$	y (in)	$\frac{u}{}$	$\frac{u}{}_r$
0.0	.32	.035	2.5	.20	.050
0.1	.29	.045	2.6	.21	.050
0.2	.30	.045	2.7	.24	.055
0.3	.32	.045	2.8	.28	.070
0.4	.30	.050	2.9	.37	.085
0.5	.28	.050	3.0	.47	.090
0.6	.27	.055	3.1	.59	.090
0.7	.24	.055	3.2	.69	.080
0.8	.22	.055	3.3	.77	.065
0.9	.19	.055	3.4	.81	.055
1.0	.17	.055	3.5	.84	.055
1.1	.16	.055	3.6	.86	.050
1.2	.14	.050	3.7	.88	.050
1.3	.12	.045	3.8	.90	.045
1.4	.11	.045	3.9	.92	.040
1.5	.10	.045	4.0	.93	.030
1.6	.09	.050	5.0	.97	.012
1.7	.09	.050	6.0	.985	.007
1.8	.10	.050	7.0	.99	.007
1.9	.10	.055	8.0	.995	.006
2.0	.12	.055	9.0	1.0	.006
2.1	.13	.060	10.0	1.0	.005
2.2	.15	.060			
2.3	.18	.055			
2.4	.20	.055			

Run 17

x/L = 0.60 T = 80°F

z/W = 0.5 q = 6.67 lbs/ft^2

D/L = 0.75

y (in)	$\frac{u}{}$	$\frac{u}{}_T$	y (in)	$\frac{u}{}$	$\frac{u}{}_T$
0.0	.34	.045	2.5	.18	.040
0.1	.32	.055	2.6	.19	.045
0.2	.34	.045	2.7	.23	.055
0.3	.32	.050	2.8	.29	0.75
0.4	.29	.055	2.9	.38	.090
0.5	.26	.055	3.0	.49	.095
0.6	.22	.055	3.1	.61	.090
0.7	.19	.050	3.2	.71	.085
0.8	.16	.045	3.3	.79	.065
0.9	.14	.040	3.4	.83	.060
1.0	.125	.035	3.5	.86	.055
1.1	.11	.035	3.6	.87	.055
1.2	.10	.035	3.7	.89	.050
1.3	.095	.035	3.8	.92	.045
1.4	.09	.035	3.9	.93	.040
1.5	.09	.040	4.0	.95	.035
1.6	.09	.040	5.0	.99	.015
1.7	.105	.040	6.0	1.0	.009
1.8	.11	.040	7.0	1.0	.008
1.9	.12	.045	8.0	1.0	.006
2.0	.13	.040	9.0	1.0	.005
2.1	.14	.040	10.0	1.0	.005
2.2	.15	.040			
2.3	.16	.040			
2.4	.17	.040			

Run 18

x/L = 0.65 T = 82°F

z/W =0.5 q = 6.67 lbs/ft^2

D/L = 0.75

y (in)	$\frac{u}{}$	$\frac{u}{}_T$	y (in)	$\frac{u}{}$	$\frac{u}{}_T$
0.0	.30	.050	2.5	.14	.045
0.1	.24	.065	2.6	.16	.050
0.2	.275	.060	2.7	.20	.060
0.3	.28	.050	2.8	.26	.080
0.4	.27	.055	2.9	.35	.095
0.5	.23	.055	3.0	.46	.100
0.6	.19	.055	3.1	.57	.100
0.7	.15	.050	3.2	.67	.090
0.8	.125	.045	3.3	.75	.075
0.9	.105	.040	3.4	.80	.065
1.0	.09	.035	3.5	.84	.055
1.1	.09	,035	3.6	.87	.055
1.2	.09	.035	3.7	.89	.050
1.3	.09	.035	3.8	.91	.045
1.4	.09	.035	3.9	.92	.040
1.5	.095	.035	4.0	.94	.040
1.6	.10	.035	5.0	.98	.015
1.7	.10	.035	6.0	.99	.009
1.8	.105	.035	7.0	.99	.007
1.9	.11	.040	8.0	.995	.007
2.0	.105	.040	9.0	1.0	.005
2.1	.11	.040	10.0	1.0	.004
2.2	.115	.045			
2.3	.12	.045			
2.4	.13	.045			

Run 19

x/L = 0.70 T = 84°F

z/W = 0.5 q = 6.67 lbs/ft^2

D/L = 0.75

y (in)	$\frac{u}{}$	$\frac{u}{}_r$	y (in)	$\frac{u}{}$	$\frac{u}{}_r$
0.0	.31	.060	2.5	.14	.050
0.1	.205	.060	2.6	.16	.060
0.2	.26	.060	2.7	.20	.070
0.3	.27	.050	2.8	.28	.085
0.4	.25	.055	2.9	.37	.100
0.5	.23	.055	3.0	.47	.100
0.6	.20	.060	3.1	.58	.100
0.7	.16	.060	3.2	.67	.090
0.8	.13	.055	3.3	.75	.080
0.9	.11	.050	3.4	.81	.065
1.0	.10	.040	3.5	.85	.060
1.1	.09	.035	3.6	.86	.055
1.2	.09	.035	3.7	.89	.050
1.3	.09	.035	3.8	.91	.045
1.4	.095	.035	3.9	.93	.045
1.5	.10	.035	4.0	.95	.035
1.6	.10	.035	5.0	.99	.012
1.7	.10	.035	6.0	1.0	.010
1.8	.105	.035	7/0	1.0	.007
1.9	.105	.035	8.0	1.0	.006
2.0	.105	.040	9.0	1.0	.005
2.1	.11	.040	10.0	1.0	.004
2.2	.11	.045			
2.3	.115	.045			
2.4	.125	.045			

Run 20

x/L = 0.75 T = 80°F

z/W = 0.5 q = 6.67 lbs/ft^2

D/L = 0.75

y (in)	$\frac{u}{}$	$\frac{u}{}_r$	y (in)	$\frac{u}{}$	$\frac{u}{}_r$
0.0	.17	.065	2.5	.14	.055
0.1	.28	.055	2.6	.17	.065
0.2	.29	.050	2.7	.23	.080
0.3	.28	.050	2.8	.30	.095
0.4	.26	.055	2.9	.39	.100
0.5	.24	.060	3.0	.50	.100
0.6	.21	.065	3.1	.60	.100
0.7	.18	.070	3.2	.68	.080
0.8	.16	.070	3.3	.75	.075
0.9	.14	.065	3.4	.80	.060
1.0	.13	.065	3.5	.84	.060
1.1	.12	.055	3.6	.86	.050
1.2	.115	.045	3.7	.88	.050
1.3	.11	.045	3.8	.90	.050
1.4	.11	.040	3.9	.92	.040
1.5	.11	.040	4.0	.94	.035
1.6	.11	.035	5.0	.975	.013
1.7	.11	.035	6.0	.99	.009
1.8	.11	.035	7.0	.99	,007
1.9	.11	.035	8.0	.99	.007
2.0	.11	.035	9.0	1.0	.006
2.1	.11	.040	10.0	1.0	.005
2.2	.11	.040			
2.3	.11	.045			
2.4	.13	.050			

Run 21

x/L = 0.80 T = 75°F

z/W =0.5 q = 6.67 lbs/ft^2

D/L = 0.75

y (in)	$\frac{u}{}$	$\frac{u}{}_T$	y (in)	$\frac{u}{}$	$\frac{u}{}_T$
0.0	.12	.060	2.5	.14	.065
0.1	.235	.045	2.6	.18	.075
0.2	.24	.045	2.7	.24	.090
0.3	.24	.050	2.8	.31	.100
0.4	.235	.055	2.9	.41	.100
0.5	.22	.065	3.0	.51	.100
0.6	.21	.070	3.1	.59	.095
0.7	.20	.075	3.2	.69	.085
0.8	.19	.080	3.3	.75	.075
0.9	.18	.080	3.4	.80	.065
1.0	.16	.080	3.5	.84	.055
1.1	.15	.075	3.6	.87	.050
1.2	.15	.075	3.7	.88	.050
1.3	.145	.065	3.8	.89	.045
1.4	.14	.060	3.9	.92	.040
1.5	.13	.055	4.0	.94	.040
1.6	.125	.055	5.0	.985	.013
1.7	.12	.045	6.0	.995	.010
1.8	.12	.040	7.0	1.0	.009
1.9	.12	.040	8.0	1.0	.007
2.0	.12	.040	9.0	1.0	.006
2.1	.11	.040	10.0	1.0	.005
2.2	.11	.040			
2.3	.11	.045			
2.4	.12	.050			

Run 22

x/L = 0.45 T = 79°F

z/W = 0.5 q = 6.67 lbs/ft^2

D/L = 0.75

y (in)	$\frac{u}{}$	$\frac{u}{}_r$	y (in)	$\frac{u}{}$	$\frac{u}{}_r$
0.0	.08	.040	2.5	.21	.055
0.1	.24	.045	2.6	.21	.055
0.2	.26	.055	2.7	.21	.060
0.3	.30	.050	2.8	.25	.075
0.4	.28	.050	2.9	.33	.090
0.5	.27	.055	3.0	.47	.090
0.6	.26	.060	3.1	.60	.095
0.7	.24	.060	3.2	.73	.075
0.8	.23	.060	3.3	.83	.060
0.9	.21	.060	3.4	.83	.060
1.0	.20	.060	3.5	.85	.055
1.1	.18	.060	3.6	.87	.050
1.2	.17	.055	3.7	.90	.045
1.3	.16	.055	3.8	.91	.045
1.4	.15	.055	3.9	.92	.040
1.5	.15	.055	4.0	.94	.035
1.6	.14	.055	5.0	.98	.014
1.7	.14	.055	6.0	.99	.011
1.8	.145	.060	7.0	1.0	.010
1.9	.155	.060	8.0	1.0	.009
2.0	.16	.060	9.0	1.0	.006
2.1	.175	.060	10.0	1.0	.006
2.2	.19	.055			
2.3	.20	.055			
2.4	.21	.050			

Run 23

x/L = 0.40 T = 82°F

z/W = 0.5 q = 6.67 lbs/ft^2

d/L = 0.75

y (in)	$\frac{u}{}$	$\frac{u}{}_r$	y (in)	$\frac{u}{}$	$\frac{u}{}_r$
0.0	.12	.055	2.5	.17	.050
0.1	.20	.050	2.6	.17	.050
0.2	.26	.055	2.7	.18	.050
0.3	.27	.055	2.8	.21	.060
0.4	.26	.055	2.9	.28	.085
0.5	.26	.060	3.0	.44	.100
0.6	.25	.060	3.1	.58	.095
0.7	.23	.060	3.2	.70	.080
0.8	.22	.065	3.3	.77	.060
0.9	.20	.065	3.4	.81	.060
1.0	.19	.060	3.5	.85	.055
1.1	.18	.060	3.6	.87	.050
1.2	.16	.065	3.7	.89	.045
1.3	.15	.060	3.8	.91	.045
1.4	.15	.055	3.9	.93	.040
1.5	.14	.055	4.0	.95	.040
1.6	.13	.055	5.0	.99	.015
1.7	.13	.055	6.0	1.0	.009
1.8	.135	.060	7.0	1.0	.008
1.9	.14	.060	8.0	1.0	.007
2.0	.15	.055	9.0	1.0	.006
2.1	.16	.055	10.0	1.0	.006
2.2	.16	.055			
2.3	.17	.050			
2.4	.17	.050			

Run 24

x/L = 0.35 T = 78°F

z/W = 0.5 q = 6.67 lbs/ft^2

D/L = 0.75

y (in)	$\frac{u}{}$	$\frac{u}{}_T$	y (in)	$\frac{u}{}$	$\frac{u}{}_T$
0.0	.15	.040	2.5	.09	.040
0.1	.08	.050	2.6	.10	.035
0.2	.20	.045	2.7	.11	.040
0.3	.20	.050	2.8	.12	.045
0.4	.19	.055	2.9	.19	.070
0.5	..8	.055	3.0	.34	.100
0.6	.17	.055	3.1	.51	.100
0.7	.15	.055	3.2	.66	.085
0.8	.14	.055	3.3	.72	.065
0.9	.12	.055	3.4	.76	.060
1.0	.11	.055	3.5	.80	.060
1.1	.10	.050	3.6	.84	.055
1.2	.09	.050	3.7	.86	.050
1.3	.08	.045	3.8	.88	.050
1.4	.075	.045	3.9	.90	.050
1.5	.07	.040	4.0	.92	.040
1.6	.07	.045	5.0	.97	.015
1.7	.08	.045	6.0	.985	.009
1.8	.08	.045	7.0	.99	.009
1.9	.09	.045	8.0	.995	.007
2.0	.09	.040	9.0	1.0	.006
2.1	.09	.040	10.0	1.0	.006
2.2	.09	.040			
2.3	.09	.040			
2.4	.09	.040			

Run 25

x/L = 0.30 T = 82°F

z/W = 0.5 q = 6.67 lbs/ft^2

D/L = 0.75

y (in)	$\frac{u}{}$	$\frac{u}{}_r$	y (in)	$\frac{u}{}$	$\frac{u}{}_r$
0.0	.18	.045	2.5	.09	.035
0.1	.16	.060	2.6	.095	.035
0.2	.18	.050	2.7	.10	.035
0.3	.20	.050	2.8	.11	.040
0.4	.20	.055	2.9	.16	.065
0.5	.18	.055	3.0	.32	.100
0.6	.17	.060	3.1	.52	.100
0.7	.16	.060	3.2	.67	.085
0.8	.14	.060	3.3	.75	.070
0.9	.13	.055	3.4	.80	.070
1.0	.12	.055	3.5	.83	.060
1.1	.11	.055	3.6	.85	.060
1.2	.10	.050	3.7	.88	.060
1.3	.10	.050	3.8	.90	.055
1.4	.09	.045	3.9	.92	.050
1.5	.08	.045	4.0	.94	.040
1.6	.08	.045	5.0	.98	.015
1.7	.08	.045	6.0	.995	.010
1.8	.09	.045	7.0	1.0	.010
1.9	.09	.045	8.0	1.0	.008
2.0	.09	.045	9.0	1.0	.006
2.1	.09	.045	10.0	1.0	.006
2.2	.09	.045			
2.3	.09	.040			
2.4	.09	.040			

Run 26

x/L = 0.25 T = 84°F

z/W =0.5 q = 6.67 lbs/ft^2

D/L = 0.75

y (in)	$\frac{u}{}$	$\frac{u}{}_r$	y (in)	$\frac{u}{}$	$\frac{u}{}_r$
0.0	.21	.055	.095	.035	
0.1	.10	.050	2.6	.10	.030
0.2	.17	.055	2.7	.10	.035
0.3	.19	.050	2.8	.11	.035
0.4	.18	.055	2.9	.17	.060
0.5	.18	.055	3.0	.34	.095
0.6	.17	.055	3.1	.56	.100
0.7	.16	.060	3.2	.69	.075
0.8	.15	.060	3.3	.75	.070
0.9	.15	.055	3.4	.80	.065
1.0	.14	.055	3.5	.83	.065
1.1	.13	.055	3.6	.88	.060
1.2	.12	.050	3.7	.88	.055
1.3	.12	.050	3.8	.90	.050
1.4	.11	.050	3.9	.92	.040
1.5	.10	.050	4.0	.93	.040
1.6	.10	.045	5.0	.985	.015
1.7	.10	.045	6.0	1.0	.011
1.8	.10	.045	7.0	1.0	.009
1.9	.10	.045	8.0	1.0	.008
2.0	.10	.040	9.0	1.0	.007
2.1	.095	.040	10.0	1.0	.006
2.2	.095	.040			
2.3	.095	.035			
2.4	.095	.035			

Run 27

x/L = 0.20 T = 86°F

z/W = 0.5 q = 6.67 lbs/ft^2

D/L = 0.75

y (in)	$\frac{u}{}$	$\frac{u}{}_T$	y (in)	$\frac{u}{}$	$\frac{u}{}_T$
0.0	.20	.055	2.5	.095	.035
0.1	.15	.060	2.6	.095	.035
0.2	.10	.060	2.7	.095	.035
0.3	.175	.055	2.8	.095	.035
0.4	.19	.050	2.9	.11	.040
0.5	.185	.055	3.0	.27	.090
0.6	.18	.055	3.1	.52	.100
0.7	.17	.055	3.2	.69	.075
0.8	.165	.055	3.3	.75	.070
0.9	.16	.055	3.4	.79	.070
1.0	.15	.050	3.5	.84	.065
1.1	.15	.055	3.6	.86	.060
1.2	.14	.055	3.7	.88	.055
1.3	.13	.055	3.8	.90	.055
1.4	.12	.050	3.9	.92	.050
1.5	.12	.050	4.0	.95	.040
1.6	.12	.045	5.0	.99	.015
1.7	.12	.045	6.0	1.0	.010
1.8	.115	.045	7.0	1.0	.009
1.9	.115	.045	8.0	1.0	.008
2.0	.11	.045	9.0	1.0	.008
2.1	.105	.045	10.0	1.0	.006
2.2	.105	.040			
2.3	.10	.040			
2.4	.10	.035			

Run 28

x/L = 0.5 T = 82°F

z/W = 0.5 q = 6.67 lbs/ft^2

D/L = 1.0

y (in)	$\frac{u}{}$	$\frac{u}{}_r$	y (in)	$\frac{u}{}$	$\frac{u}{}_r$
0.0	.36	.050	2.5	.07	.055
0.1	.35	.050	2.6	.09	.060
0.2	.28	.070	2.7	.11	.060
0.3	.25	.055	2.8	.12	.060
0.4	.23	.050	2.9	.135	.055
0.5	.22	.050	3.0	.155	.055
0.6	.21	.050	3.1	.16	.050
0.7	.19	.050	3.2	.17	.050
0.8	.17	.050	3.3	.175	.045
0.9	.15	.050	3.4	.18	.040
1.0	.125	.045	3.5	.19	.040
1.1	.11	.045	3.6	.19	.040
1.2	.09	.040	3.7	.20	.040
1.3	.08	.035	3.8	.23	.055
1.4	.07	.030	3.9	.29	.075
1.5	.065	.030	4.0	.40	.100
1.6	.05	.025	5.0	.94	.040
1.7	.045	.025	6.0	.98	.015
1.8	.04	.025	7.0	.995	.011
1.9	.04	.025	8.0	1.0	.010
2.0	.04	.030	9.0	1.0	.009
2.1	.04	.035	10.0	1.0	.008
2.2	.04	.035	11.0	1.0	.006
2.3	.05	.045			
2.4	.06	.050			

Run 29

x/L = 0.2 T = 84°F

z/W = 0.5 q = 6.67 lbs/ft^2

D/L = 1.00

y (in)	$\frac{u}{}$	$\frac{u}{}_T$	y (in)	$\frac{u}{}$	$\frac{u}{}_T$
0.0	.17	.085	2.5	.20	.050
0.1	.18	.055	2.6	.20	.050
0.2	.135	.050	2.7	.195	.050
0.3	.15	.045	2.8	.19	.045
0.4	.16	.045	2.9	.19	.045
0.5	.165	.040	3.0	.185	.045
0.6	.165	.045	3.1	.18	.040
0.7	.17	.045	3.2	.18	.040
0.8	.17	.045	3.3	.18	.035
0.9	.175	.045	3.4	.16	.035
1.0	.18	.045	3.5	.15	.035
1.1	.18	.045	3.6	.145	.035
1.2	.18	.045	3.7	.135	.035
1.3	.18	.045	3.8	.15	.045
1.4	.18	.045	3.9	.27	.080
1.5	.18	.045	4.0	.49	.100
1.6	.18	.045	5.0	.94	.040
1.7	.18	.045	6.0	.99	.015
1.8	.18	.050	7.0	1.0	.010
1.9	.18	.050	8.0	1.0	.009
2.0	.18	.050	9.0	1.0	.008
2.1	.19	.055	10.0	1.0	.006
2.2	.19	.055	11.0	1.0	.006
2.3	.195	.055			
2.4	.20	.050			

Run 30

x/L = 0.25 T = 72°F

z/W = 0.5 q = 6.67 lbs/ft^2

D/L = 1.00

y (in)	$\frac{u}{}$	$\frac{u}{}_r$	y (in)	$\frac{u}{}$	$\frac{u}{}_r$
0.0	.10	.050	2.5	.19	.050
0.1	.10	.055	2.6	.195	.050
0.2	.13	.045	2.7	.19	.050
0.3	.15	.045	2.8	.19	.050
0.4	.16	.045	2.9	.19	.045
0.5	.17	.040	3.0	.185	.045
0.6	.17	.040	3.1	.185	.040
0.7	.17	.045	3.2	.18	.040
0.8	.17	.045	3.3	.185	.038
0.9	.17	.045	3.4	.18	.035
1.0	.17	.045	3.5	.18	.035
1.1	.17	.045	3.6	.18	.035
1.2	.17	.045	3.7	.175	.035
1.3	.17	.045	3.8	.18	.040
1.4	.17	.045	3.9	.24	.065
1.5	.17	.045	4.0	.39	.095
1.6	.17	.045	5.0	.93	.035
1.7	.17	.045	6.0	.97	.015
1.8	.17	.045	7.0	.98	.009
1.9	.17	.045	8.0	.99	.008
2.0	.175	.050	9.0	.995	.007
2.1	.18	.050	10.0	1.0	.006
2.2	.18	.055	11.0	1.0	.006
2.3	.18	.055			
2.4	.19	.050			

Run 31

z/L = 0.3 T = 78°F

z/W = 0.5 q = 6.67 lbs/ft^2

D/L = 1.00

y (in)	$\frac{u}{}$	$\frac{u}{}_r$	y (in)	$\frac{u}{}$	$\frac{u}{}_r$
0.0	.14	.055	2.5	.18	.055
0.1	.13	.070	2.6	.18	.055
0.2	.15	.040	2.7	.18	.050
0.3	.16	.045	2.8	.18	.050
0.4	.17	.045	2.9	.18	.050
0.5	.17	.040	3.0	.18	.045
0.6	.17	.045	3.1	.18	.045
0.7	.17	.045	3.2	.18	.040
0.8	.17	.045	3.3	.18	.040
0.9	.17	.045	3.4	.18	.035
1.0	.165	.045	3.5	.18	.035
1.1	.165	.045	3.6	.18	.035
1.2	.165	.045	3.7	.18	.035
1.3	.16	.045	3.8	.18	.037
1.4	.16	.045	3.9	.22	.055
1.5	.159	.045	4.0	.34	.085
1.6	.155	.045	5.0	.93	.035
1.7	.155	.045	6.0	.975	.015
1.8	.155	.045	7.0	.99	.009
1.9	.155	.050	8.0	.99	.009
2.0	.155	.050	9.0	.995	.007
2.1	.16	.055	10.0	1.0	.006
2.2	.17	.055	11.0	1.0	.005
2.3	.17	.055			
2.4	.18	.055			

Run 32

x/L = 0.35 T = 80°F

z/W = 0.5 q = 6.67 lbs/ft^2

D/L = 1.0

y (in)	$\underline{u}$	$\underline{u}_r$	y (in)	$\underline{u}$	$\underline{u}_r$
0.0	.27	.050	2.5	.155	.060
0.1	.22	.065	2.6	.16	.060
0.2	.19	.050	2.7	.17	.055
0.3	.195	.045	2.8	.18	.055
0.4	.19	.045	2.9	.175	.050
0.5	.19	.045	3.0	.175	.050
0.6	.185	.045	3.1	.175	.045
0.7	.175	.050	3.2	.175	.045
0.8	.17	.050	3.3	.18	.040
0.9	.165	.050	3.4	.18	.040
1.0	.155	.050	3.5	.19	.037
1.1	.15	.050	3.6	.19	.035
1.2	.14	.048	3.7	.19	.035
1.3	.13	.045	3.8	.20	.045
1.4	.125	.045	3.9	.26	.070
1.5	.12	.045	4.0	.39	.095
1.6	.115	.045	5.0	.94	.040
1.7	.115	.045	6.0	.98	.015
1.8	.115	.050	7.0	.995	.010
1.9	.11	.050	8.0	1.0	.008
2.0	.12	.055	9.0	1.0	.007
2.1	.13	.060	10.0	1.0	.006
2.2	.135	.060	11.0	1.0	.006
2.3	.145	.065			
2.4	.15	.060			

Run 33

x/L = 0.4 T = 81°F

z/W = 0.5 q = 6.67 lbs/ft^2

D/L = 1.0

y (in)	$\frac{u}{}$	$\frac{u}{}_r$	y (in)	$\frac{u}{}$	$\frac{u}{}_r$
0.0	.24	.055	2.5	.14	.060
0.1	.16	.045	2.6	.145	.060
0.2	.20	.045	2.7	.15	.055
0.3	.20	.045	2.8	.15	.050
0.4	.20	.045	2.9	.155	.050
0.5	.19	.045	3.0	.165	.050
0.6	.18	.050	3.1	.16	.050
0.7	.175	.050	3.2	.17	.045
0.8	.16	.050	3.3	.17	.045
0.9	.15	.055	3.4	.175	.040
1.0	.13	.050	3.5	.18	.040
1.1	.12	.050	3.6	.19	.040
1.2	.105	.045	3.7	.20	.040
1.3	.105	.045	3.8	.225	.055
1.4	.095	.040	3.9	.30	.080
1.5	.085	.040	4.0	.43	.100
1.6	.08	.040	5.0	.93	.040
1.7	.08	.040	6.0	.97	.015
1.8	.08	.040	7.0	.98	.009
1.9	.08	.045	8.0	.99	.008
2.0	.08	.050	9.0	.99	.008
2.1	.095	.055	10.0	1.0	.008
2.2	.105	.060	11.0	1.0	.007
2.3	.115	.060			
2.4	.125	.060			

Run 34

x/L = 0.45 T = 84°F

z/W = 0.5 q = 6.67 lbs/ft^2

D/L = 1.0

y (in)	$\frac{u}{}$	$\frac{u}{}_r$	y (in)	$\frac{u}{}$	$\frac{u}{}_r$
0.0	.32	.050	2.5	.10	.065
0.1	.30	.050	2.6	.12	.065
0.2	.20	.055	2.7	.13	.060
0.3	.22	.050	2.8	.14	.060
0.4	.215	.045	2.9	.145	.055
0.5	.21	.050	3.0	.15	.050
0.6	.205	.050	3.1	.15	.050
0.7	.19	.055	3.2	.155	.045
0.8	.18	.055	3.3	.16	.045
0.9	.15	.055	3.4	.165	.040
1.0	.14	.055	3.5	.17	.040
1.1	.125	.050	3.6	.175	.040
1.2	.11	.050	3.7	.185	.045
1.3	.10	.045	3.8	.22	.055
1.4	.09	.040	3.9	.30	.085
1.5	.085	.040	4.0	.42	.100
1.6	.075	.040	5.0	.95	.040
1.7	.065	.035	6.0	.99	,015
1.8	.06	.035	7.0	.995	.015
1.9	.06	.035	8.0	1.0	.010
2.0	.06	.040	9.0	1.0	.010
2.1	.065	.045	10.0	1.0	.008
2.2	.07	.050	11.0	1.0	.007
2.3	.08	.055			
2.4	.085	.060			

Run 35

x/L = 0.55 T = 78°F

z/W = 0.5 q = 6.67 lbs/ft^2

D/L = 1.0

y (in)	$\frac{u}{}$	$\frac{u}{}_T$	y (in)	$\frac{u}{}$	$\frac{u}{}_T$
0.0	.29	.050	2.5	.015	.020
0.1	.26	.055	2.6	.02	.025
0.2	.235	.050	2.7	.03	.040
0.3	.24	.045	2.8	.05	.045
0.4	.24	.045	2.9	.08	.055
0.5	.23	.045	3.0	.105	.060
0.6	.22	.045	3.1	.13	.060
0.7	.21	.045	3.2	.155	.050
0.8	.19	.045	3.3	.17	.045
0.9	.17	.045	3.4	.185	.040
1.0	.15	.045	3.5	.20	.040
1.1	.135	.040	3.6	.20	.040
1.2	.12	.035	3.7	.22	.045
1.3	.10	.030	3.8	.26	.070
1.4	.09	.030	3.9	.34	.090
1.5	.075	.025	4.0	.45	.095
1.6	.065	.025	5.0	.94	.045
1.7	.055	.025	6.0	.97	.020
1.8	.05	.025	7.0	.985	.010
1.9	.045	.025	8.0	.99	.007
2.0	.035	.020	9.0	.99	.007
2.1	.03	.020	10.0	1.0	.006
2.2	.025	.020	11.0	1.0	.005
2.3	.02	.017			
2.4	.015	.015			

Run 36

x/L = 0.6 T = 80°F

z/L = 0.5 q = 6.67 lbs/ft^2

D/L = 1.0

y (in)	$\frac{u}{}$	$\frac{u}{}_r$	y (in)	$\frac{u}{}$	$\frac{u}{}_r$
0.0	.27	.055	2.5	.025	.020
0.1	.24	.070	2.6	.03	.025
0.2	.22	.050	2.7	.039	.030
0.3	.23	.050	2.8	.05	.040
0.4	.225	.050	2.9	.07	.050
0.5	.22	.050	3.0	.09	.055
0.6	.215	.050	3.1	.12	.055
0.7	.20	.050	3.2	.14	.050
0.8	.18	.050	3.3	.17	.045
0.9	.16	.045	3.4	.18	.040
1.0	.14	.040	3.5	.19	.040
1.1	.12	.035	3.6	.215	.040
1.2	.11	.035	3.7	.225	.050
1.3	.095	.030	3.8	.28	.070
1.4	.085	.027	3.9	.36	.090
1.5	.075	.027	4.0	.46	.100
1.6	.065	.025	5.0	.94	.040
1.7	.06	.025	6.0	.985	.015
1.8	.05	.025	7.0	.995	.009
1.9	.045	.025	8.0	1.0	.008
2.0	.04	.023	9.0	1.0	.007
2.1	.04	.020	10.0	1.0	.007
2.2	.03	.020	11.0	1.0	.006
2.3	.03	.020			
2.4	.025	.020			

Run 37

x/L = 0.65 T = 84°F

z/W = 0.5 q = 6.67 lbs/ft^2

D/L = 1.0

y (in)	$\frac{u}{}$	$\frac{u}{}_r$	y (in)	$\frac{u}{}$	$\frac{u}{}_r$
0.0	.26	.060	2.5	.045	.030
0.1	.19	.080	2.6	.05	.030
0.2	.18	.060	2.7	.05	.035
0.3	.20	.055	2.8	.07	.040
0.4	.21	.055	2.9	.08	.050
0.5	.215	.055	3.0	.10	.050
0.6	.21	.055	3.1	.115	.050
0.7	.19	.055	3.2	.135	.050
0.8	.17	.050	3.3	.155	.045
0.9	.15	.050	3.4	.17	.045
1.0	.13	.045	3.5	.18	.040
1.1	.115	.040	3.6	.20	.045
1.2	.10	.035	3.7	.22	.060
1.3	.09	.035	3.8	.27	.080
1.4	.08	.035	3.9	.36	.095
1.5	.075	.030	4.0	.46	.100
1.6	.07	.030	5.0	.95	.045
1.7	.07	.030	6.0	.99	.015
1.8	.06	.030	7.0	1.0	.011
1.9	.06	.030	8.0	1.0	.009
2.0	.055	.030	9.0	1.0	.008
2.1	.05	.025	10.0	1.0	.006
2.2	.05	.025	11.0	1.0	.006
2.3	.045	.025			
2.4	.045	.025			

Run 38

x/L = 0.65 T = 82°F

z/W = 0.5 q = 6.67 lbs/ft^2

D/L = 1.0

y (in)	$\frac{u}{}$	$\frac{u}{}_r$	y (in)	$\frac{u}{}$	$\frac{u}{}_r$
0.0	.25	.055	2.5	.04	.030
0.1	.20	.080	2.6	.045	.030
0.2	.19	.055	2.7	.05	.040
0.3	.21	.055	2.8	.06	.040
0.4	.215	.055	2.9	.075	.045
0.5	.215	.055	3.0	.09	.050
0.6	.215	.055	3.1	.11	.050
0.7	.20	.050	3.2	.13	.050
0.8	.175	.050	3.3	.15	.045
0.9	.15	.045	3.4	.165	.040
1.0	.13	.040	3.5	.18	.040
1.1	.115	.035	3.6	.19	.045
1.2	.095	.035	3.7	.22	.055
1.3	.085	.035	3.8	.26	.075
1.4	.08	.030	3.9	.35	.090
1.5	.07	.030	4.0	.45	.100
1.6	.07	.030	5.0	.94	.045
1.7	.065	.030	6.0	.99	.015
1.8	.055	.030	7.0	.995	.012
1.9	.055	.027	8.0	1.0	.010
2.0	.05	.027	9.0	1.0	.008
2.1	.05	.025	10.0	1.0	.006
2.2	.045	.025	11.0	1.0	.006
2.3	.045	.025			
2.4	.04	.025			

Run 39

x/L = 0.75 T = 84°F

z/W = 0.5 q = 6.67 lbs/ft^2

D/L = 1.0

y (in)	$\frac{u}{}$	$\frac{u}{}_T$	y (in)	$\frac{u}{}$	$\frac{u}{}_T$
0.0	.04	.040	2.5		
0.1	.10	.060	2.6	.10	.030
0.2	.13	.090	2.7	.10	.030
0.3	.16	.060	2.8	.10	.035
0.4	.17	.060	2.9	.105	.035
0.5	.18	.060	3.0	.11	.035
0.6	.19	.055	3.1	.115	.040
0.7	.18	.060	3.2	.12	.040
0.8	.16	.055	3.3	.125	.040
0.9	.14	.055	3.4	.135	.045
1.0	.13	.055	3.5	.15	.050
1.1	.12	.055	3.6	.17	.060
1.2	.11	.050	3.7	.22	.080
1.3	.105	.050	3.8	.28	.095
1.4	.10	.045	3.9	.37	.105
1.5	.10	.040	4.0	.47	.105
1.6	.10	.040	5.0	.94	.040
1.7	.10	.035	6.0	.99	.015
1.8	.10	.035	7.0	1.0	.010
1.9	.10	.035	8.0	1.0	.008
2.0	.10	.030	9.0	1.0	.007
2.1	.10	.030	10.0	1.0	.006
2.2	.10	.030	11.0	1.0	.006
2.3	.10	.030			
2.4	.10	.030			

Run 40

x/L = 0.8 T = 82°F

z/W = 0.5 q = 6.67 lbs/ft^2

D/L = 1.0

y (in)	$\frac{u}{}$	$\frac{u}{}_T$	y (in)	$\frac{u}{}$	$\frac{u}{}_T$
0.0			2.5	.13	.030
0.1			2.6	.125	.030
0.2			2.7	.125	.030
0.3	.14	.055	2.8	.12	.030
0.4	.15	.060	2.9	.12	.030
0.5	.165	.060	3.0	.115	.030
0.6	.175	.060	3.1	.115	.035
0.7	.175	.060	3.2	.11	.035
0.8	.16	.060	3.3	.11	.040
0.9	.15	.065	3.4	.12	.045
1.0	.14	.065	3.5	.13	.055
1.1	.135	.065	3.6	.16	.070
1.2	.13	.065	3.7	.21	.090
1.3	.13	.060	3.8	.28	.100
1.4	.125	.055	3.9	.36	.110
1.5	.125	.055	4.0	.46	.110
1.6	.125	.050	5.0	.95	.040
1.7	.13	.045	6.0	.985	.013
1.8	.13	.045	7.0	.995	.010
1.9	.13	.040	8.0	1.0	.009
2.0	.13	.040	9.0	1.0	.006
2.1	.13	.040	10.0	1.0	.006
2.2	.13	.035	11.0	1.0	.006
2.3	.13	.030			
2.4	.13	.030			

INITIAL DISTRIBUTION LIST

		No. Copies
1.	Defense Documentation Center Cameron Station Alexandria, Virginia 22314	20
2.	Library Naval Postgraduate School Monterey, California	2
3.	Professor Louis Schmidt (Thesis Advisor) Department of Aeronautics Naval Postgraduate School Monterey, California	1
4.	Lt. Roger Lee Bennett, USN Staff, Com Des Ron 6 FPO New York, New York 09501	1
5.	Department of Mechanical Engineering (Files) Naval Postgraduate School Monterey, California	1

DOCUMENT CONTROL DATA - R&D

(Security classification of title, body of abstract and indexing annotation must be entered when the overall report is classified)

1. ORIGINATING ACTIVITY (Corporate author)	2a. REPORT SECURITY CLASSIFICATION
Naval Postgraduate School Monterey, California	Unclassified
	2b. GROUP

3. REPORT TITLE

An Experimental Investigation of Standing Vortices in an Open Cavity

4. DESCRIPTIVE NOTES (Type of report and inclusive dates)

5. AUTHOR(S) (Last name, first name, initial)

Bennett, Roger L., LT, USN

6. REPORT DATE	7a. TOTAL NO. OF PAGES	7b. NO. OF REFS
June 1967	86	12

8a. CONTRACT OR GRANT NO.	9a. ORIGINATOR'S REPORT NUMBER(S)
b. PROJECT NO.	
c.	9b. OTHER REPORT NO(S) (Any other numbers that may be assigned this report)
d.	

10. AVAILABILITY/LIMITATION NOTICES

[redacted]

11. SUPPLEMENTARY NOTES	12. SPONSORING MILITARY ACTIVITY
	Naval Postgraduate School Monterey, California

13. ABSTRACT

This report describes the measurement of velocity profiles within and directly above a rectangular cavity with air flow across its mouth, such that standing vortices are induced in the cavity. The constant temperature hot-wire anemometer was used to determine velocity profiles at 75 feet per second free stream velocity and cavity depth over length ratios of 0.75 and 1.0. Both three-dimensional and cavity geometry effects were exhibited for the vortices, and lack of periodicity in the velocities was consistently noted.

All of the experimental work was conducted during April and May 1967, at the Naval Postgraduate School.

DD FORM 1 JAN 64 1473

14. KEY WORDS	LINK A		LINK B		LINK C	
	ROLE	WT	ROLE	WT	ROLE	WT
Hydrodynamics						
Standing Vortices						
Cavity Resonance